เซลล์แสงอาทิตย์ชนิดสีย้อมไวแสงที่มีชั้นอิเล็กโตรดชนิด Al_2O_3/TiO_2 หรือ MgO/TiO_2

นางสาวจีราภา ธรรมสนิท

วิทยานิพนธ์นี้เป็นส่วนหนึ่งของการศึกษาตามหลักสูตรปริญญาวิศวกรรมศาสตรมหาบัณฑิต
สาขาวิชาวิศวกรรมเคมี ภาควิชาวิศวกรรมเคมี
คณะวิศวกรรมศาสตร์ จุฬาลงกรณ์มหาวิทยาลัย
ปีการศึกษา 2553

DYE-SENSITIZED SOLAR CELL WITH Al_2O_3/TiO_2 OR MgO/TiO_2 ELECTRODE LAYER

Miss Jeerapa Tammasanit

A Thesis Submitted in Partial Fulfillment of the Requirements

for the Degree of Master of Engineering Program in Chemical Engineering

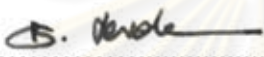Department of Chemical Engineering

Faculty of Engineering

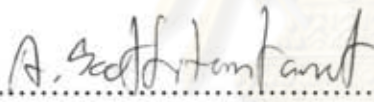Chulalongkorn University

Academic Year 2010

Thesis Title	DYE-SENSITIZED SOLAR CELL WITH Al_2O_3/TiO_2 OR MgO/TiO_2 ELECTRODE LAYER
By	Miss Jeerapa Tammasanit
Field of Study	Chemical Engineering
Thesis Advisor	Akawat Sirisuk, Ph.D.

Accepted by the Faculty of Engineering, Chulalongkorn University in Partial Fulfillment of the Requirements for the Master's Degree
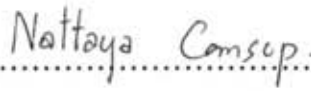
....Dean of the Faculty of Engineering

(Associate Professor Boonsom Lerdhirunwong, Dr.Ing.)

THESIS COMMITTEE

....Chairman

(Apinan Soottitantawat, Ph.D.)

....Thesis Advisor

(Akawat Sirisuk, Ph.D.)

....Examiner

(Assistant Professor Joongjai Panpranot, Ph.D.)

....External Examiner

(Nattaya Comsup, D. Eng)

จีราภา ธรรมสนิท : เซลล์แสงอาทิตย์ชนิดสีย้อมไวแสงที่มีชั้นอิเล็กโตรดชนิด Al_2O_3/TiO_2
หรือ MgO/TiO_2 (DYE-SENSITIZED SOLAR CELL WITH Al_2O_3/TiO_2 OR MgO/TiO_2
ELECTRODE LAYER) อ. ที่ปรึกษาวิทยานิพนธ์หลัก: อ.ดร.อัครวัต ศิริสุข, 67 หน้า.

งานวิจัยนี้ทำการศึกษาประสิทธิภาพของเซลล์แสงอาทิตย์ชนิดสีย้อมไวแสงที่มีชั้น
อิเล็กโตรดเป็นไทเทเนียมไดออกไซด์เติมด้วยอะลูมินาและแมกนีเซียมออกไซด์   โดยปริมาณใน
การเติมอะลูมินาและแมกนีเซียมออกไซด์ทำในช่วงร้อยละ 0 ถึง 2 โดยน้ำหนัก สังเคราะห์ขึ้นด้วย
วิธีโซล-เจล และพ่นเคลือบลงบนกระจกนำไฟฟ้าด้วยเครื่องพ่นอัลตร้าโซนิค ความหนาของชั้น
ฟิล์มที่พ่นเคลือบประมาณ 10 ไมโครเมตร เซลล์แสงอาทิตย์ชนิดสีย้อมไว แสงที่ทำการเติมอะลูมิ
นาร้อยละ 1 โดยน้ำหนัก ในไทเทเนียมไดออกไซด์ซึ่งถูกเผาที่ 400 องศาเซลเซียส มีประสิทธิภาพ
ของเซลล์แสงอาทิตย์สูงสุดที่ร้อยละ 5.04 จากผลของจุดไอโซอิเล็กทริคที่พีเอชเพิ่มขึ้น การเติม
อะลูมินาทำให้จุดไอโซอิเล็กทริคสูงขึ้น ส่งผลให้พื้นผิวดูดซับโมเลกุลสีย้อมได้ดีขึ้น การเพิ่มขึ้นที่
นำไปสู่การเพิ่มขึ้นของความหนาแน่นของกระแสไฟฟ้าลัดวงจร   และประสิทธิภาพของเซลล์แสง
อาทิตย์ที่สูงขึ้น   เมื่อเปรียบเทียบกับเซลล์แสงอาทิตย์ชนิดชั้นอิเล็กโตรดที่มีไทเทเนียมไดออกไซด์
เพียงอย่างเดียว ในทางกลับกันการเติมแมกนีเซียมไดออกไซด์ทำให้จุดไอโซอิเล็กทริค มีค่าลดลง
ปริมาณการดูดซับสีย้อมลดลง   ส่งผลให้ค่าความหนาแน่นของกระแสไฟฟ้าลัดวงจรและ
ประสิทธิภาพของเซลล์แสงอาทิตย์ลดลง   เมื่อศึกษาผลของอุณหภูมิในการเผาชั้นอิเล็กโตรดของ
อะลูมินากับไทเทเนียมไดออกไซด์คอมโพสิต พบว่าประสิทธิภาพของเซลล์ลดลง เนื่องจากเฟสอะ
นาเทสเปลี่ยนเป็นเฟสรูไทล์มากขึ้น   และพื้นที่ผิวลดลง   จากนั้นทำการศึกษาผลของชั้นฟิล์ม
อิเล็กโตรดแบบสองชั้น พบว่าประสิทธิภาพของเซลล์เพิ่มขึ้นเป็นร้อยละ 5.50 เมื่อเปรียบเทียบกับ
ชั้นอิเล็กโตรดแบบชั้นเดียว ที่พื้นที่ผิวใกล้เคียงกัน ชั้นอิเล็กโตรดแบบสองชั้น ทำให้มีการกระเจิง
ของแสงมากขึ้น ส่งผลให้แสงถูกสะท้อนกลับไปยังชั้นของสีย้อมมากขึ้น ซึ่งเห็นได้จากสเปกตรัม
การสะท้อนกลับของแสง

ภาควิชา... ...วิศวกรรมเคมี...............ลายมือชื่อนิสิต.............จีราภา ธรรมสนิท.............
สาขาวิชา......วิศวกรรมเคมี...............ลายมือชื่อ อ.ที่ปรึกษาวิทยานิพนธ์หลัก..............
ปีการศึกษา...2553............

##5270244921: MAJOR CHEMICAL ENGINEERING

KEYWORDS: DYE-SENSITIZED SOLAR CELL/ SPRAY COATING / TiO_2/ SOL-GEL METHOD

JEERAPA TAMMASANIT: DYE-SENSITIZED SOLAR CELL WITH Al_2O_3/TiO_2 OR MgO/TiO_2 ELECTRODE LAYER. ADVISOR : AKAWAT SIRISUK, Ph.D.,67 pp.

This research investigated the performance of dye-sensitized solar cells with composite Al_2O_3/TiO_2 and MgO/TiO_2 electrode layer. The amount of Al_2O_3 or MgO added was in the range of 0 to 2 % (w/w). The composite mixture was synthesized by sol-gel methods and sprayed onto the conducting glass by an ultrasonic spray coater. The thickness of the film was approximately 10 μm. Dye sensitized solar cells with an electrode of 1 % (w/w) Al_2O_3 and TiO_2 that was sintered at 400°C yielded the highest efficiency of 5.04%. The addition of alumina increased an isoelectric point of the mixture, resulting in greater amount of dye molecules being adsorbed on the surface. This increase led to improved short circuit current density and higher efficiency of the cells when compared to cells with pure TiO_2 electrode. On the other hand, the addition of magnesium oxide lowered an isoelectric point of the mixture, thereby decreasing the amount of dye adsorbed. This decrease led to smaller short circuit current density and lower efficiency of the cell. When the sintering temperature of composite Al_2O_3/TiO_2 electrode increased, the efficiency dropped because anatase phase was converted to the rutile phase and surface area was decreased. When a double-layered Al_2O_3/TiO_2 electrode was employed, the efficiency of the solar cell increased to 5.50% when compared to a single-layered Al_2O_3/TiO_2 electrode with similar specific surface area. Double-layered TiO_2 electrode increased the light scattering, resulting in more light reflected back to dye layer, as evident in diffused reflectance spectrum.

Department:............Chemical Engineering.....Student's Signature......*Jeerapa Tammasanit*

Field of Study:........Chemical Engineering.....Advisor's Signature...

Academic Year:.....2010.............

ACKNOWLEDGEMENTS

This thesis would not have been possible to complete without the support of the following individuals. Firstly, I would like to express my greatest gratitude to my advisor, Dr. Akawat Sirisuk, for his invaluable guidance during the course of this work. And I am also very grateful to Dr. Apinan Soottitantawat, thesis committee chairman, and other committee members, Assistant Professor Joongjai Panpranot and Dr. Nattaya Comsup, from Pathumwan Institute of Technology.

Many thanks for kind suggestions and useful assistance from scientists at NECTEC for I-V tester measurement and many friends at the Center of Excellence on Catalysis and Catalytic Reaction Engineering, who always provide the encouragement and assistance along the study. To the many others, not specifically named, who have provided me with support and encouragement, please be assured that I think of you.

Finally, I also would like to dedicate this thesis to my parents, my brother and my sister, who have always been the source of my support and encouragement.

CONTENTS

LIST OF TABLES

LIST OF FIGURES

ศูนย์วิทยทรัพยากร
จุฬาลงกรณ์มหาวิทยาลัย

CHAPTER I

INTRODUCTION

Among the alternative energy resources, the solar energy is more notable because of its low environmental impact. Therefore, the research on photovoltaic cell has attracted considerable interest. Particularly, the dye-sensitized solar cell (DSSC) proposed by O'Regan and Grätzel (O'Regan and Gratzel., 1991) have attracted much attention since 1991. The dye-sensitized solar cell (DSSC) based on nanoporous TiO_2 electrodes divectly convert sunlight into electrical energy. This is attributed to its properties, low manufacturing cost, relatively high energy conversion efficiencies, easy fabrication, portability and flexibility when compared to conventional silicon solar cells (Green et al., 2007). To date, the highest solar to electric conversion efficiency of over 11% was achieved using a photoelectrode containing 20 nm TiO_2 nanoparticles film sensitized by a ruthenium-based dye (Gratzel et al., 2003).

The dye-sensitized solar cell (DSSC) possesses three major components: (i) nanostructured metal oxide material to transport electrons efficiently, (ii) dye sensitizer in order to harvest solar energy and generate excitons, and (iii) redox electrolyte or hole transporting material, to support the performance of dye and metal oxide (Thavasi et al., 2009). Many efforts have been made to improve the energy conversion efficiency of the dye-sensitized solar cell (DSSC) by developing novel photoelectrodes, dyes, and electrolytes (Jung et al., 2010). The photoactive electrode of the dye-sensitized solar cell (DSSC) is a transparent conductive oxide glass coated with nanoporous TiO_2 sensitized with dyes for visible light harvesting, while the counter electrode is a transparent conductive oxide glass coated with platinum. The gap between the two electrodes is filled with an electrolyte containing an iodide/tri-iodide (I^-/I_3^-) redox couple. The TiO_2 electrode in the dye-sensitized solar cell (DSSC) has a large surface area and provides sufficient anchoring sites for the dye sensitizers to provide effective light harvesting and electron injection. However, electron transfer from ruthenium complex dye does not work perfectly because many electrons recombine with the holes at the interface between TiO_2 and the electrolyte. Efficient

operation of the dye-sensitized solar cell (DSSC) device relies on minimization of the possible recombination pathways occurring at the TiO_2|dye|electrolyte interface.

In order to reduce the recombination, many researchers have proposed devices that include the use of insulating metal oxides with higher band gaps such as MgO (Jung et al., 2005), Al_2O_3 (Liu et al., 2005), SrO (Yang et al., 2002), Nb_2O_5 (Xia et al., 2007), $CaCO_3$ (Lee et al., 2007), and $MgTiO_3$ (Yang et al., 2009) between the TiO_2 and the dye interface. Recently, Ganapathy and coworkers. (2010) proposed that the modification of TiO_2 by Al_2O_3 using atomic layer deposition could increase the efficiency of dye-sensitized solar cells. A layer of Al_2O_3 on TiO_2 surface reduced the loss of electrons by suppressing their recombination, resulting in a significant increase in the short-circuit current and the overall power conversion efficiency.

This research focuses mainly on improving the power conversion efficiency for dye-sensitized solar cells through modification of TiO_2 electrode. Another oxide, namely, Al_2O_3 or MgO, was mixed with TiO_2 sol and the thin film mixed oxide electrode is prepared. The effects of several preparation parameters on the cell efficiency were investigated, including the calcination temperature and the double-layer structure.

Objectives

1. To enhance the efficiency of a dye-sensitized solar cell by adding Al_2O_3 or MgO to the TiO_2 electrode.
2. To study of the effect of calcination temperature of Al_2O_3/TiO_2 electrode layer on the efficiency of a dye-sensitized solar cell.
3. To improve efficiency of a dye-sensitized solar cell by employing double-layer structure of the thin film electrode.

Research scopes

Part I

- Titanium dioxide (TiO_2), Al_2O_3 and MgO is prepared by sol-gel methods.
- Al_2O_3 or MgO is added to TiO_2 in the amount ranging from 0 to 2 % (w/w).
- The mixed oxide electrode is characterized by several techniques.
    o X-ray diffractometry (XRD)
    o Nitrogen physisorption
    o UV-visible diffuse reflectance spectroscopy
    o Inductively coupled plasma optical emission spectrophotometer
    o Zeta potential measurement
    o Fourier Transform Infrared Spectroscopy (FT-IR)
- The efficiency of dye-sensitized solar cell is measured by an I-V tester.

Part II

- Study the effect of calcination temperature of the dye-sensitized solar cells with mixed oxide electrode from Part I on their efficiencies.
- Study the effect of using double-layer thin film electrode that possesses similar specific surface area to that of a single-layer one.
- Characterize the electrode and the cell using several techniques already mentioned in Part I.

This thesis is arranged as follows:

Chapter I presented the introduction of this study.

Chapter II presented the structure and operation principles of dye-sensitizer solar cell (DSSC).

Chapter III presented the literature reviews of previous works related to this research.

Chapter IV presented the synthesis of the TiO_2 sol and modified TiO_2 via sol-gel methods.

Chapter V presented and discussed experimental results.

In the last chapter. Chapter VI presented overall conclusion and recommendations for the future studies.

CHAPTER II

THEORY

Dye-sensitized solar cell (DSSC)

The dye sensitized solar cell (DSSC) mainly consists of light sensitive dyes, porous layer of TiO_2 (wide band gap semiconductor), redox electrolyte, front and back electrodes made of transparent conducting oxide (FTO). At the heart of the system is a mesoporous oxide layer composed of nanometer-sized particles which have been sintered together to allow for electronic conduction to take place. The material of choice has been TiO_2 (anatase) although alternative wide band gap oxides such as ZnO, and Nb_2O_5 have also been investigated.

The principle of DSSC is the photoexcitation of dye resulting in electron injection into the conduction band of the metal oxide (MO), hole injection into the electrolyte, and gets reduced as shown below (Thavasi et al,. 2009):

$$Dye^{+-} + MO \xrightarrow{\text{electron injection}} Dye^+ + MO^- \qquad (2.1)$$
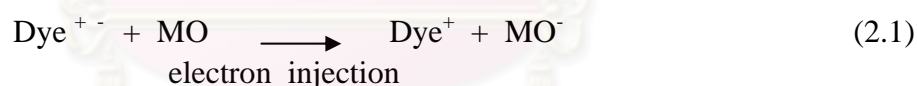
Redox species, usually comprises of iodide/triiodide redox couple, in the electrolyte transport the holes from the oxidized dye to the counter electrode. In the absence of redox species, the injected electrons from excited state of dye undergo recombination with oxidized dye, instead of iodine.

$$Dye^+ + MO^- \xrightarrow{\text{recombination with dye}} Dye + MO \qquad (2.2)$$
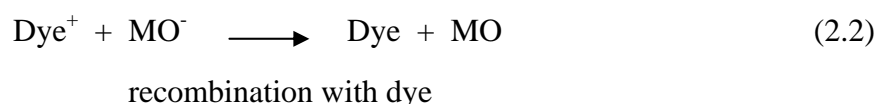
The redox electrolyte prevents the reduced dye recapturing the injected electron by donating its own electron and thus regenerates the reduced dye.

$$Dye^+ + 2I^- \xrightarrow{\text{dye regeneration}} Dye + I_2^- \qquad (2.3)$$
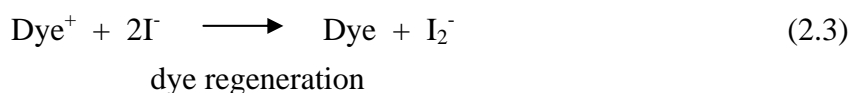
The oxidized iodide is then regenerated by the triiodide at the counter electrode, with the electrical circuit being completed via electron migration through the external load.

$$I_2^- + MO^- \longrightarrow 2I^- + MO \qquad (2.4)$$

iodide regeneration
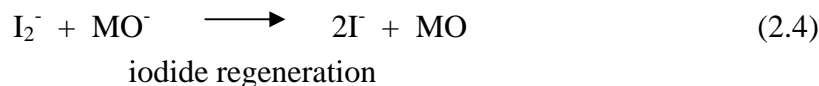
Back electron transfer from metal oxide into the electrolyte is however the primary and predominant recombination pathway in DSSC, which lower the conversion efficiency.

$$I_2^- + MO^- \longrightarrow 2I^- + MO \qquad (2.5)$$

recombination with electrolyte
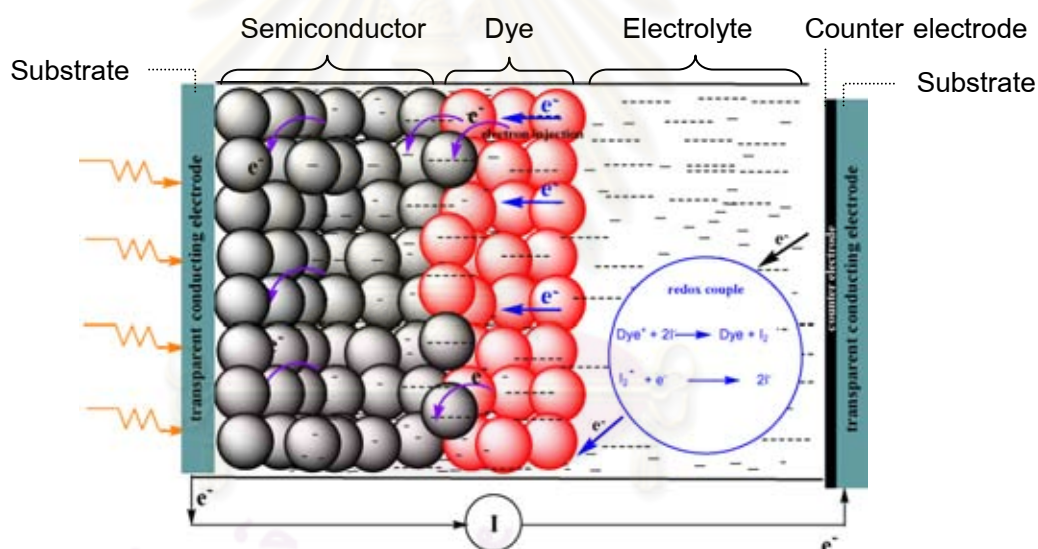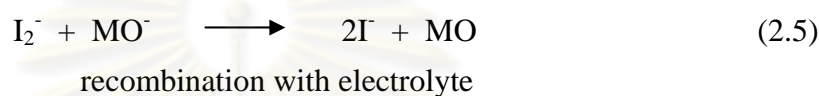
Figure 2.1 Schematic diagram of dye sensitized solar cells (Thavasi et al., 2009)

The performance of each components is crucial and have been designated using the parameters: open-circuit voltage Voc, fill factor FF and short circuit current density Jsc and expressed as efficiency (η) using the equation:

$$\eta = \frac{V_{OC} J_{SC} FF}{P_{in}} \qquad \text{and} \qquad FF = \frac{I_{max} V_{max}}{J_{SC} V_{OC}}$$

Whereas   Voc, is the maximum voltage obtained at zero current.

Jsc, the shot circuit current is the maximum current obtained under less resistance (short circuit) condition.

P_{in} is the solar radiation intensity.

I_{max} and V_{max} are the maximum current and maximum voltage, respectively.

2.1 Components of DSSC

2.1.1 Photosensitized

The best photovoltaic performance both in terms of conversion yield and long-term stability has so far been achieved with polypyridyl complexes of ruthenium and osmium. Sensitizers having the general structure ML2 (X) 2, where L stands for 2,2'-bipyridyl-4,4'-dicarboxylic acid M is Ru or Os and X presents a halide, cyanide, thiocyanate, acetyl acetonate, thiacarbamate or water substituent, are particularly promising.

The amount of the sensitizer molecules available for light harvesting and charge injection are important upon adsorbing dye onto the metal oxide. Dye molecules are to be oriented on the surface of metal oxide with attachment functionalities of the molecule. Orientation reduces the covering area per adsorbed molecule, providing a more compact and packed arrangement of the dye molecules, which allow for more adsorption dye of molecules. The rate constant for the migration of the excited energy would depend on the relative orientation of the donor and acceptor moieties. However, this is no longer possible if the dye is adsorbed as aggregates. Problem of poor electron transfer to the metal oxide conduction band would be arisen if dyes are aggregated that results in an unsuitable energetic position of the LUMO level. Lower current density could be resulted by poor injection efficiency, due to unfavourable binding of dye onto the metal oxide surface. The orientation of the molecule on the metal oxide surface is characterized by the anchoring group present in the dye (Rochfoed et al., 2007). Anchoring groups of dye to the semiconductor surface is the most decisive factor help in bringing the relative

orientation of energy level of donor and acceptor during the attachment on the metal oxide and increase injection efficiency. Thus, the ruthenium complex *cis*-RuL$_2$(NCS)$_2$, known as N3 dye, shown in Figure 2.2 has become the paradigm of heterogeneous charge transfer sensitizer for mesoporous solar cells.

The fully protonated N3 has absorption maxima at 518 and 380 nm, the extinction coefficients being 1.3 and 1.33 $\times$ 10^{4}M^{-1}cm^{-1}, respectively. The optical transition has metal-to-ligand charge transfer (MLCT) character: excitation oft the dye involves transfer of an electron from the metal to the p* orbital of the surface anchoring carboxylated bipyridyl ligand from where it is released within femto- to picoseconds into the conduction band of TiO$_2$ generating electric charges with unit quantum yield (Grätzel., 2003).
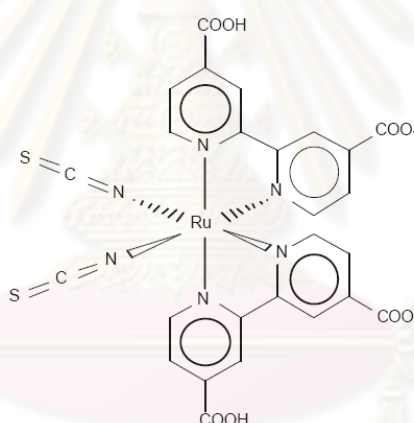
Figure 2.2 Chemical structure of the N3 ruthenium complex used as a charge transfer sensitizer in dye-sensitized solar cells. (Gratzel., 2003)
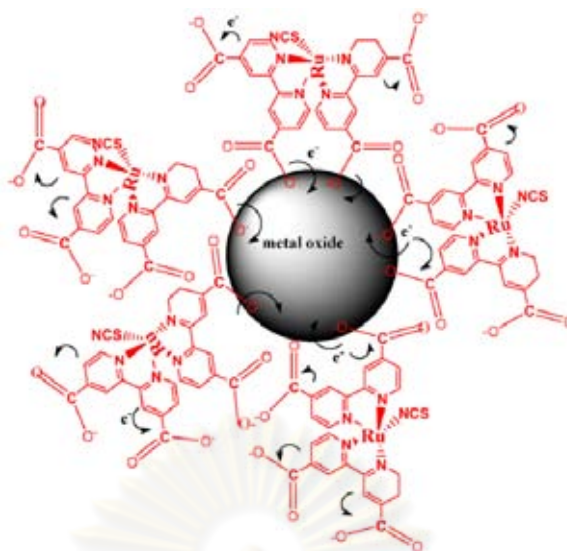
Figure 2.3 Inefficient electron injection into metal oxide arises from misalignment
and higher degree of protonation in N3 dye. (Thavasi et al., 2009)

N3 dye has two bipyridine ligands and four carboxyl groups in its structure
and adsorption may occur via several modes viz. protonation of one or more of all the
four carboxyl groups (Nazeeruddin et al., 2003), which results in difference in their
energy levels that in turn lead to differences in their electron injection efficiency. For
example, the fully protonated N3 dye, while possessing an excellent light-harvesting
capability, shows poor electron injection efficiency due to the misalignment of the
dye on TiO_2 (Figure 2.3) (Nilsing et al., 2007).

2.1.2 TiO_2 electrode film

Nano-porous TiO_2 thin films have been widely used as the working electrodes
in dye-sensitized solar cells (DSSC). In DSSC, titanium dioxide (TiO_2) is one of the
most promising materials used for nano-porous thin film due to its appropriate energy
levels, dye adsorption ability, low cost, and easy preparation (Hsiue , 2010).

Titanium dioxide (TiO_2) is a wide band gap ($\sim$3.2 eV for the anatese phase)
semiconductor material which has been under extensive investigations due to its
applications in a variety of fields such as photoelectrolysis (Mishra et al., 2003),
photocatalysis (Yu et al., 2001) comprise dye sensitized solar cells (Ko et al., 2005).
TiO_2 has 3 crystalline forms: anatase, rutile and brookite. Many important

applications of TiO_2 depend on its structural and optical properties. The anatase phase gained much attention due to its more active surface chemistry and smaller particles for more dye adsorption, which has better response with ultraviolet photons is used for photocatalysis (Yu et al., 2001). Anatase is metastable and can be transformed irreversibly to thermodynamically more stable and condense rutile phase at higher temperature. The rutile phase has good stability and high refractive index which makes it suitable for protective coatings on lenses (Takikawa et al., 1999). Rutile to anatase transformation occurs in the temperature range 700-1000°C depending on the crystallite size and impurity content. The band gap energies for anatase and rutile have been estimated to be 3.2 and 3.0 eV, respectively.

Titanium oxide films have been made by a variety of techniques such as e-beam evaporation, magnetron sputtering technique, anodization, chemical vapour deposition (CVD) and sol gel technique. Among the different methods for the preparation of thin TiO_2 layer, sol-gel technique is widely used because of its low processing cost, simplicity and ability to produce thin and uniform films on large area substrates (Mathews et al., 2009).

The sol-gel conventional method uses the hydrolytic route, which involves the initial hydrolysis of the alkoxide precursor followed by continual condensations between the hydrolysed particles forming the gel. The hydrolysis and the polycondensation of titanium alkoxides proceed according to the following scheme (Harizanov et al., 2000):

$$M\text{-}O\text{-}R + H_2O \longrightarrow M\text{-}OH + R\text{-}OH \qquad \text{Hydrolysis reaction} \qquad (2.6)$$

$$M\text{-}OH + HO\text{-}M \longrightarrow M\text{-}O\text{-}M + H_2O \qquad \text{Water condensation} \qquad (2.7)$$

$$M\text{-}O\text{-}R + HO\text{-}M \longrightarrow M\text{-}O\text{-}R + R\text{-}OH \qquad \text{Alcohol condensation} \qquad (2.8)$$

Then, M   substitute the semiconductor material sach as Si, Zr, Ti, Al, Sn or Ce

OR   substitute the alkoxyl group

2.1.3 Counter electrode performance

Solar cell studies employ usually a Fluorine dope tin oxide (FTO) as the conducting glass electrode. Such electrodes are known to be poor choice for efficient reduction of triiodide. To reduce the overvoltage losses, a very fine Pt-layer or islands of Pt is deposited on to the conducting glass electrode. This ensures high exchange current densities at the counter-electrode and thus the processes at the counter electrode do not become rate limiting in the light energy harvesting process (Kalyanasundaram et al., 1998).

2.2 Structure and operation principles of dye-sensitizer solar cell

The primary processes in dye-sensitized solar cells. At the heart of the system is a nanocrystalline mesoporous TiO_2 film with a monolayer of the charge transfer dye attached to its surface. The film is placed in contact with a redox electrolyte or an organic hole conductor. Photoexcitation of the sensitizer dye (process (1) in Figure 2.4), the electrons are injected from the excited sensitizer dyes into the conduction band (CB) of the semiconductor film (electron injection) (process (2) in Figure 2.4). The injected electrons recombine with the oxidized sensitizer dyes (recombination). This recombination process competes with the regeneration of the oxidized sensitizer dyes by the redox mediator molecules (rereduction). The electrons can be transported in the semiconductor film as the conducting electrons. The conducting electrons can react with the redox mediator molecules or with molecules in the solution during transport, before reaching the back contact electrode (leak reaction). Finally, the remaining electrons flow into the external circuit (Katoh et al., 2004).
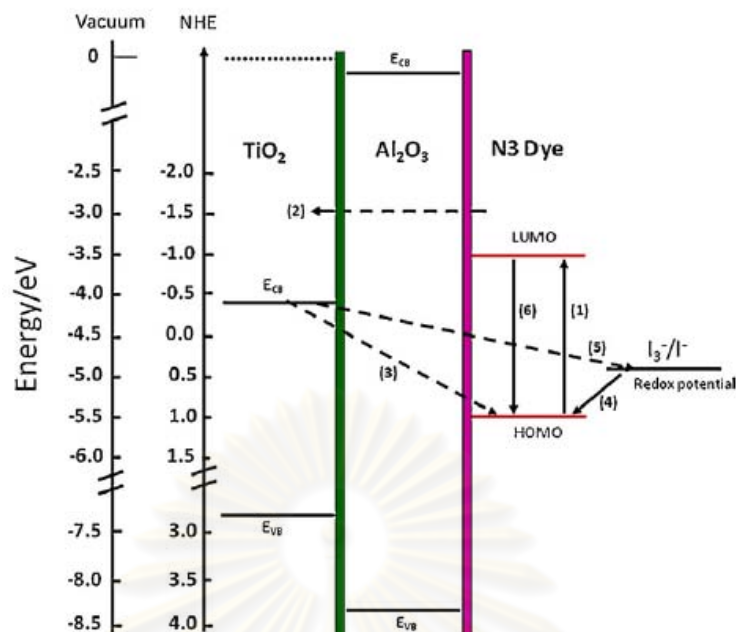
Figure 2.4 Schematic diagram of band structure including interfacial charge-transfer
processes occurring at TiO_2|dye|electrolyte interface in dye-sensitized
solar cells. (Ganapathy et al., 2010)

Efficient operation of a DSSC device relies on minimization of the possible
recombination pathways occurring at the TiO_2|dye|electrolyte interface to allow
efficient charge transport through the TiO_2 porous layer and subsequent charge
collection at the device contacts. The energy band structure at the TiO_2|dye interface
where charge separation processes take place in a DSSC with photon illumination is
illustrated in Figure 2.4. There are two possible recombination losses to consider. The
photo-generated electrons may recombine either with oxidized dye molecules
(process (3) in Figure 2.4) or with the oxidized redox couple (process (5) in Figure
2.4); the latter reaction is thought to be particularly critical to the device performance.
In order to reduce the recombination, many groups have proposed device architectures
that include the use of insulating polymers (Gregg et al., 2001), high band-gap
semiconductor metal oxides like ZnO and Nb_2O_5. Also the use of insulating metal
oxides such as $CaCO_3$, $BaTiO_3$, MgO and Al_2O_3 between the TiO_2 and the dye
interface has been attempted.

CHAPTER III

LITERATURE REVIEWS

This chapter presents the literature reviews for dye-sensitized solar cell (DSSC)

3.1 Modification of TiO$_2$ electrode with mixed-metal oxides

To improve the performance of solar cells, one effective approach is the interfacial modification of nanoporous TiO$_2$ films with high band-gap semiconductor metal oxide coating layer such as SrO, SrTiO$_3$, CaCO$_3$, Nb$_2$O$_5$, MgO and Al$_2$O$_3$ between the TiO$_2$ and the dye interface has been attempted. MgO and Al$_2$O$_3$ have been studied as an insulating barrier given its high conduction band edge compared with TiO$_2$. Recently, many groups have proposed as follows;

Luo and coworkers (2008) studied, dye-sensitized TiO$_2$ electrodes were immersed into a solution of aluminum isopropoxide (Al$_2$O$_3$ over layer, Figure 3.1) using a "wet-chemical" method and after hydrolysis quasi-solid-state solar cell were fabricated. The cells with Al$_2$O$_3$ coating shown lower back current and better performance: under low light intensity illumination, the Voc increased by ~50mV, the Jsc decreased a little, and the overall efficiency was improved slightly; under 100mW·cm^{-2} AM 1.5, both the Voc and Jsc increased, resulting in a significant 28% improvement in overall efficiency. The Al$_2$O$_3$ coating also resulted in better stability of solar cells without encapsulation due to depression of the dye desorption and electrolyte degradation.
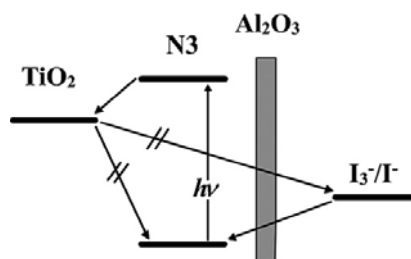
Figure 3.1 Illustration of the interfacial charge transfer processes occurring at the TiO$_2$|dye|electrolyte of a DSSC. Also shown is the Al$_2$O$_3$ overlayer as developed in this study. (Luo et al., 2008)

Bandara and coworkers (2008) investigated how the MgO coating on TiO$_2$ and SnO$_2$ affect of the flat-band (FB) potential levels. The results of coating of a thin insulating MgO layer on TiO$_2$ or SnO$_2$ particles to decreased a back-electron transfer reaction rate and can be assumed that the MgO coating on TiO$_2$ and SnO$_2$ may change the charge transfer and recombination kinetics which may in turn enhance the solar cell performance and photocatalytic activity.

Yang and coworkers (2002) preparation of nanoporous TiO$_2$ electrodes modified with an MgTiO$_3$ layer (represented as TiO$_2$/MgTiO$_3$) and its application in dye-sensitized solar cells (DSSC). The conduction band of MgTiO$_3$ stands higher than that of TiO$_2$, so the MgTiO$_3$ layer can be beneficial to the improvement of nanoporous TiO$_2$ electrodes. nanoporous TiO$_2$ films were prepared from colloids with particles of about 20 nm diameter. The surface modified TiO$_2$/MgTiO$_3$ electrode was fabricated by dipping a TiO$_2$ thin film in 0.2 mol·L^{-1} MgCl$_2$ and TiCl$_4$ mixture aqueous solution and sintered in air at 450°C for 30 minute. As a result, the photoelectrochemical properties of the modified electrodes were improved and the overall energy conversion efficiency η was increased from 6.12% to 8.75% under the illumination of a white light of 100 mW/cm^2.

Ganapathy and coworkers (2010) studied Alumina (Al$_2$O$_3$) shell formation on TiO$_2$ core nanoparticles by atomic layer deposition (ALD) to suppress the

recombination of charge carriers generated in a dye-sensitized solar cell (DSSC). ALD is an efficient process for controlling the nanostructure and layer thickness by regulating the number of deposition cycles. For a porous TiO_2 later prepared by applying a paste of TiO_2 nanoparticles (Ti Nanoxide T20) by means of a doctorblade on the FTO glass substrates and then annealing at 450°C for 30 minute. Then, the alumina coated TiO_2 electrodes and immediately immersed in solution of N3 dye. After the analyzed, a layer of Al_2O_3 on TiO_2 surface reduces the loss of electrons by suppressing their recombination, and this results in a significant increase in the short-circuit current and the overall power conversion efficiency.

César and coworkers (2010) preparation and characterization of core-shell electrodes for application in gel electrolyte-based dye-sensitized solar cells. The TiO_2 electrodes were prepared from TiO_2 powder (P25 Degussa) and coated with thin layers of Al_2O_3, MgO, Nb_2O_5 and $SrTiO_3$ prepared by the sol-gel method. The improvement in the solar cell energy conversion efficiency by the overcoat approach may be assigned to the following factors: (i) the wide band gap coating delays the electron back transfer to the electrolyte and minimizes charge recombination, (ii) the coating layer also enhances the dye adsorption onto the porous electrode and, as a consequence, the dye loading, increasing the photocurrent. The optimum performance was achieved by solar cells based on MgO/TiO_2 core-shell electrode: fill factor of ~0.60, short-circuit current density Jsc of 12 mA·cm^{-2}, open-circuit voltage Voc of 0.78 V and overall energy conversion efficiency of ~5% (under illumination of 100 mW·cm^{-2}).

Bihui and coworkers (2010) studied MgO/TiO_2 core shell film was obtained by using a simple chemical bath deposition method to coat a thin MgO film around TiO_2 nanoparticals. After 20 minute dipping of MgO, Jsc is increased by 19.6% from 7.36 mA·cm^{-2} to 8.80 mA·cm^{-2}, and η is increased by 21.8% from 4.32% to 5.26%. The increase of the FF and η of the solar cell is due to the formed energy barrier by the thin MgO layer. Moreover, the MgO coating promotes the dye molecular adsorption ability of the electrodes, leading to the improvement of the Jsc.

However, the use of mixed metal oxide as an electrode was an alternative approach to enhance the efficiency of DSSC.

3.2 The structure of TiO$_2$ electrode of the dye-sensitized solar cell

Lee and coworkers (2009) investigated the improvement of the DSSC performance afforded by using multi-layered TiO$_2$ electrodes by light-scattering effect. Three types of TiO$_2$ electrode (shown in Fig 3.2) of the DSSC device were composed of TiO$_2$ particles of 9 nm, 20 nm, and 123 nm in the average diameter. The use of the light-scattering layers resulted in an increase of the Jsc value, thus the overall power conversion efficiency by 6.03% under illumination of simulated AM 1.5 solar light (100 mW·cm^{-2}) was attained with a multi-layer structure using 123-nm-TiO$_2$ layer for the light-scattering layer and 9-nm-TiO$_2$ layer for the dense layer.

Xu and coworkers (2009) prepared bilayer-structured film with TiO$_2$ nanocrystals as underlayer and TiO$_2$ nanotubes as overlayer. The resultant double-layer TiO$_2$ film could significantly improve the efficiency of dye-sensitized solar cell owing to its synergic effects, i.e. effective dye adsorption mainly originated from TiO$_2$ nanocrystal layer and rapid electron transport in one-dimensional TiO$_2$ nanotube layer. The overall energy conversion efficiency of 6.15% was achieved by the formation of double layer TiO$_2$ film, with is 44.70% higher than that formed by pure nanocrystalline TiO$_2$ film. It is expected that the double layer film electrode can be extended to other composite film with different layer structures and morphologies for enhancing the efficiencies of DSSC.
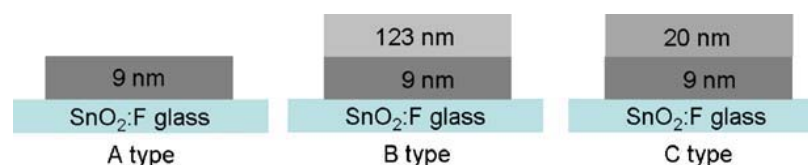
Figure 3.2 Three types of TiO$_2$ electrode onto SnO$_2$:F glass prepared for dye-sensitized solar cells. (From Lee et al., 2009)

CHAPTER IV

EXPERIMENTAL

This chapter discusses various material and method employed in this research. The experiments involved (i) preparation of TiO_2 film and metal oxide dope TiO_2 film, and measuring their characteristics. (ii) preparation of dye-sensitized solar cell components. (iii) assembled the DSSC by fit: the working electrode, the counter electrode and the electrolyte, and (iv) physical and electrochemical characterization.

4.1 Preparation of TiO_2 film and metal oxide dope TiO_2 film

The preparation of the TiO_2 film and metal oxide dope TiO_2 film consisted of two steps: the preparation of TiO_2 sol via sol gel method and the application of TiO_2 sol onto electrode by ultrasonic spray coating.

4.1.1 Preparation of TiO_2 sol

TiO_2 sol was prepared via a sol-gel method. A solution consisted of 14.44 ml of 70% nitric acid and 2000 ml of distilled water. Titanium (IV) isopropoxide in the amount of 166.80 ml was added slowly into the solution while being stirred continuously at room temperature. The mixture solution was stirred for 3-4 days until clean sol was obtained. Next, the clean sol underwent dialysis in a cellulose membrane. The distilled water used for dialysis was changed daily until a pH of 3.5 was obtained. And then, TiO_2 sol was kept in a refrigerator until needed.

4.1.2 Preparation of metal oxide dope TiO_2 sol

In this work , another oxide was added to TiO_2 film. The metal oxide chosen for this study were Al_2O_3 and MgO , which were added to a TiO_2 sol at concentrations of 0.25%, 1.0% and 2.0% (w/w).

4.1.2.1 Preparation of Al_2O_3/TiO_2 sol

To prepare Al_2O_3 sol, one mixed 2 g of aluminium iso-propoxide [AIP] in 44 ml of deionized water, which had been preheated to about 90°C. After the solution had been stirred thoroughly for one hour, 1.2 ml of 1 M HCl was added (the molar ratio of AIP : water : HCl is 1: 100: 0.05). Then the solution was stirred at 90°C for another hour. An almost transparent sol was.

To obtain 0.25%, 1.0% and 2.0% (w/w) of Al_2O_3/TiO_2 mixture, one mixed 0.43 ml, 1.71 ml and 3.42 ml of Al_2O_3 sol, respectively, with 80.44 ml, 79.84 ml and 79.03 ml of TiO_2 sol, respectively. The solution was stirred until homogeneity was obtained. Then, the mixture solution underwent dialysis in a cellulose membrane until a pH of 3.5 was obtained.

4.1.2.2 Preparation of MgO/TiO_2 sol

Preparation of MgO sol, this work mixed Magnesium nitrate hexahydrate $[Mg(NO_3)_2 \cdot 6H_2O]$ and Oxalic acid $[(COOH)_2 \cdot 2H_2O]$ precursors in 1:1 molar ratio are first dissolved separately in ethanol and stirred to obtain two clear solutions.

To obtain 0.25%, 1.0% and 2.0% (w/w) of MgO/TiO_2, this work mixed 0.21 ml, 0.83 ml and 1.66 ml of magnesium sol with TiO_2 sol with the volume of 80.44 ml, 79.84 ml and 79.03 ml respectively. The solution was stirred until homogeneity was obtained. Add then, the mixture solution underwent dialysis in a cellulose membrane until a pH 3.5 was obtained.

4.2 Preparation of dye-sensitized solar cell components and the fabrication procedure

The components of DSSC are mainly considered of transparent conducting glass, dye, electrolyte, counter electrode and anode electrode.

4.2.1 Transparent conducting oxide glass

The conducting glass is transparent conducting oxide coated glass, which is the fluorine-doped tin oxide (FTO) coated on electrically conducting glass. The glass was purchased from Solaronix (Switzerland) under the commercial name TCO22-15. To identify the conducting side of fluorine doped tin oxide coated on glass, one used a multimeter to measure resistance. The conducting side would have a sheet resistance of ca. 15-20 ohm. The glass was cleaned with ethanol and dried with a hair-dryer.

4.2.2 Dye sensitized

In this research, this work employed Cis-di(thiocyanate)bis(2,2'-bipyridine-4,4'-dicarboxylate)ruthenium (II) or N3 (R535) dye from Solaronix, which was widely used in dye-sensitized solar cell. To prepare the dye solution, 20 mg of N3 dye was dissolved in 100 ml of ethanol and the mixture was stirred until a homogeneous solution was obtained. The resulting product was a solution of 0.3 mM N3 dye in ethanol.

4.2.3 Electrolyte

Electrolyte consisted of 0.5 M lithium iodine (LiI), 0.05 M iodide (I_2), and 0.5 M 4-tert-butylpyridine (TBP) in acetronitrile, one mixed 2.00 g of LiI, 0.38 g of I_2, and 2.20 ml of TBP in 30 ml of acetronitrile. The solution was stirred until homogeneity was obtained.

4.2.4 Counter electrode

The counter electrode for the DSSC was platinum coated on conducting glass. To prepare a platinum counter electrode by ion sputtering, one first cut a conducting glass to a rectangular piece that was 1.0×1.5 cm^2 in site. The glass was cleaned with ethanol was dried with a hair-dryer. Then, tape was placed on one side of the glass as seen in Figure 4.1. Wipe off any fingerprints using a tissue wet with ethanol. Then, platinum target was sputtering on the conducting glass using ion sputtering (JEOL
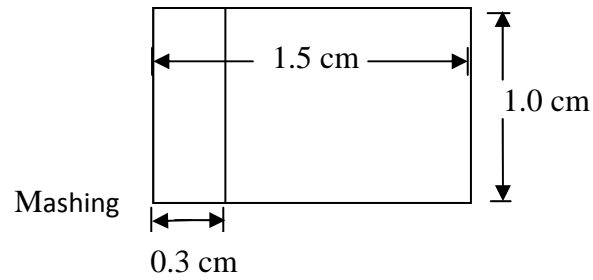
Figure 4.1 The counter electrode before sputtering

JFC-1100E) at 10 mA of ion current for four minutes. After sputtering, masking tape was removed.

4.2.5 Anode electrode

Anode electrode consisted of TiO_2 film or metal oxide dope TiO_2 film on a conducting glass. To prepare the anode electrode, first we cut a conducting glass into a rectangular piece that was 1.0×1.5 cm^2. The glass clean with ethanol and dry with a hair-dryer. Then the glass was masked with aluminum foil to a circle have radius 0.5 cm as seen in Figure 4.2. The cut out was located closer to one side of the foil than the other.
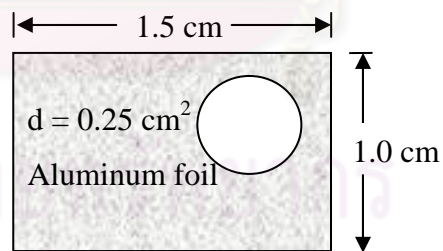
Figure 4.2 The anode electrode before spray coating

After masking, TiO_2 was coated on the conducting glass using ultrasonic spray coater. Stir well the TiO_2 sol before use, not shake unless bubbles could be formed. The spraying liquid such as TiO_2 sol was placed in a syringe pump, which fed the liquid at a rate 1 ml/min to an ultrasonic nozzle. The level speed of a moving stage was 4. The power of an ultrasonic nozzle, provided by a frequency generator until was 3.5 watts.

This study effect of modified TiO_2 electrode then this work controlled the number of coats of TiO_2 sol, Al_2O_3/TiO_2 sol or MgO/TiO_2 sol at 500 coats. After a few coats, TiO_2 thin film was dried by a hair dryer. The thickness of film was measured using profilmeter (Veeco Dektak 150). The anode electrode was sintered at 400°C for two hours. After anode electrodes was left to be cooled to 30°C. Before dye impregnation, we heat electrode on hotplate at 70°C for 10 minute, to avoid water absorption. Put slowly the anode electrode was immersed in a solution of 0.3 mM N3 dye for 12 hours in the dark. Then, the anode electrode rinsed with ethanol (The ethanol remove water from the porous TiO_2) and dye with hair-dryer. Finally, the anode electrodes were assembled.

4.3 Assembled and tested the DSSC

Assembly the two electrodes (counter and anode electrode), First this work cut two strips of a sealing material that were 0.15 cm wide and 1.2 cm long. The strips were inserted as spacer between the platinum counter electrode and anode electrode. The platinum counter electrode was placed on top of the anode electrode so that the conducting side of the counter electrode was on top of the TiO_2 film. The cell was sealed by heating the sealing material with a hotplate at 60°C for 3 minute (see Figure 4.3)

The platinum counter electrode

Sealing material $\longrightarrow$ $\longleftarrow$ Sealing material

Anode electrode
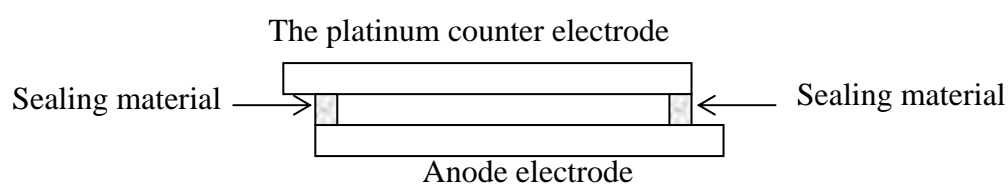
Figure 4.3 Cross-section of assembled dye solar cell showing sealing rim
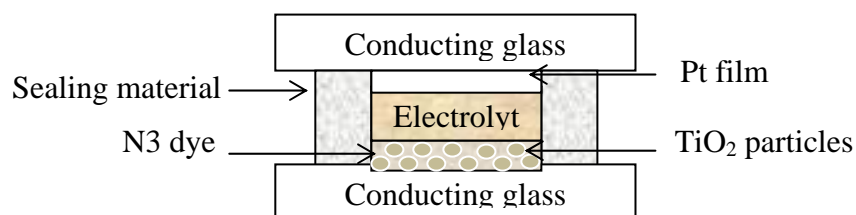
Figure 4.4 Fabrication of dye-sensitized solar cell assembly for testing

For electrolyte filling, in cell having a sealing rim with two small holes, the filling is done by putting a droplet onto only one hole, and let it soak up (see Figure 4.4), then clean carefully the area around the filling holes with acetone. The cell is ready for testing.

4.4 Physical and electrochemical characterization

In this section discussed various techniques for physical and electrochemical properties of TiO_2, metal oxide dope TiO_2 and dye sensitized, various characterization techniques were employed.

4.4.1 X-ray diffractometry (XRD)

XRD was performed to determine crystal phase and crystallite size of TiO_2, Al_2O_3/TiO_2 and MgO/TiO_2. It was conducted using a SIEMENS D5000 X-ray diffractometer with Cu K_α radiation (λ= 1.54439Å) with Ni filter. The spectra were scanned at a rate of 0.04 min^{-1} in the 2θ range of 20-80°.

4.4.2 Nitrogen physisorption

To determine the specific surface area of TiO_2, Al_2O_3/TiO_2 and MgO/TiO_2 were measured through nitrogen gas adsorption in a continuous flow method at liquid nitrogen temperature. A mixture of nitrogen and helium was employed as the carrier

gas using Micromeritics ChemiSorb 2750 Pulse Chemisorption Ststem instrument. The sample was thermally treated at 200°C for one hour before measurement.

4.4.3 UV-Visible Absorption Spectroscopy (UV-Vis)

To determine the amount of dye adsorption was determine by a spectroscopic method by measuring the concentration of dye desorbed on the titania film into a mixed solution of 0.1M NaOH and ethanol (1:1 in volume fraction). The absorption spectra by UV-Vis Absorption Spectroscopy (Perkin Elmer Lampda 650, λ between 300-800 nm and step size 1 nm).

4.4.4 Inductively Coupled Plasma-Atomic Emission Spectroscopy (ICP-AES)

The amount of metal deposited on the surface of titanium dioxide (TiO_2) was measured with an Optima 2100 DV spectrometer. The sample was solution, we dissolved 0.01 g of catalyst in 5 ml of 49% hydrofluoric acid (Merck) stirred until homogenous solution then the solution make to 100 ml with deionized water. The solution has concentration of 5 ppm ($mg \cdot l^{-1}$) from the catalyst which was assumed to have metal content of 2.0 wt %.

4.4.5 Zeta potential measurement

Zeta potential measurement were carried out on ZetaPlus (Malvern/Zetasizer), which uses the Doppler shift resulting from laser light scatter from the particles to obtain a mobility spectrum. A sample was suspended in deionized water and the pH of the suspension was adjusted using a 0.1M HCl and NaOH solution.

4.4.6 Fourier Transform Infrared Spectroscopy (FT-IR)

FT-IR analysis of modified TiO_2 was carried out in a Nicolet model 6700 of the IR spectrometer using the wavenumber ranging from 400-4000 cm^{-1} with a resolution of 4 cm^{-1}.

4.4.7 Current-Voltage Tester (I-V Tester)

The electrochemical properties of dye-sensitized solar cell were determined by I-V tester Current-Voltage measurements were performed using white light source under air mass (AM) 1.5G condition. To determine current density, open circuit voltage, cell resistance, and fill factor. This information was then converted to efficiency of the solar cell. An area of our solar cell was 0.196 cm^2. The equipment used was MV systems Inc., Xenon short ARC (Osram XBO 1000 W/HS).

The performance of each components is crucial and have been designated using the parameters: open-circuit voltage Voc, fill factor FF and short circuit current density Isc and expressed as efficiency (η) using the equation:

$$\eta = \frac{V_{OC} J_{SC} FF}{P_{in}} \tag{4.1}$$

and

$$FF = \frac{I_{max} V_{max}}{J_{SC} V_{OC}} \tag{4.2}$$

whereas ;   Voc, is the maximum voltage obtained at zero current

Jsc, the shot circuit current is the maximum current obtained under less resistance (short circuit) condition

P_{in} is the solar radiation intensity.

I_{max} and V_{max} are the maximum current and maximum voltage, respectively

CHAPTER V

RESULTS AND DISCUSSION

In this chapter, the experimental results and discussion were described and divided into three major parts, namely, influence of mixed of Al_2O_3 and MgO to TiO_2 electrode layer, influence of sintering temperature and influence of double-layer structure of the thin film electrode on the performance of dye sensitized solar cell.

5.1 Effect of modification of TiO_2 electrode layer

5.1.1 Modification of TiO_2 electrode layer by adding Al_2O_3

TiO_2 electrode later was modified by addition of Al_2O_3 to electrode at the percentage of Al_2O_3/TiO_2 was 0.25 wt %, 1.0 wt % and 2.0 wt %, the electrode calcined at 400°C for 120 minutes and the number of coats were 500 coats have film thickness was approximately 10.5 µm which sinter temperature and the thickness gave highest the efficiency of dye sensitized solar cell, this work study influence of percentage of Al_2O_3/TiO_2 on performance of dye sensitized solar cell.

XRD patterns for the Al_2O_3/TiO_2 composite and bare TiO_2 are shown in Figure 5.1. It is apparent that the crystalline form of TiO_2 is anatase, rutile and brookite phase. It has been reported that anatase phase has higher photocatalytic oxidation-reduction activity than rutile phase. The band gap energies for anatase phase and rutile phase have been estimated to be 3.2 and 3.0 eV, respectively (Chen et al., 2010). The results from XRD showed that weight fraction of anatase phase increases when the mixing of Al_2O_3 increases (see in Table 5.1). The added alumina oxide role was based on the crystal growth inhibiter, which leading to small grain size correlated with high surface area (see in Table 5.1).

The amount of Al on Ti catalyst was determined using inductively coupled plasma atomic emission spectroscopy (ICP-AES). From ICP analysis the ratio of Al_2O_3/TiO_2 atomic ratio of Al_2O_3-TiO_2 mixed oxide calcined at 400°C for 120

minutes showed in Table 5.1. From result of ICP analysis found that the contents of Al less than the nominal value may because the preparation of mixed oxide sol.
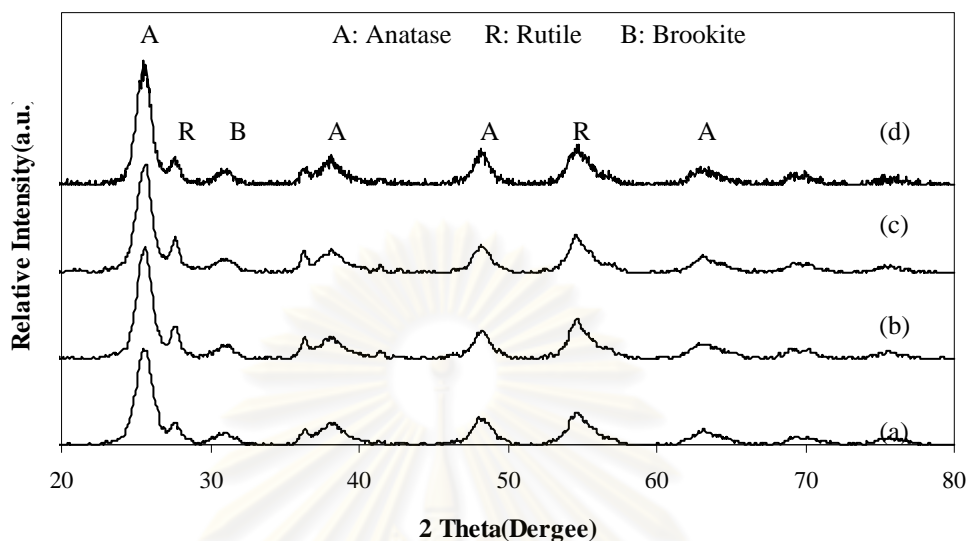
Figure 5.1 XRD patterns of Al_2O_3/TiO_2 powders at various percentages of
Al_2O_3/TiO_2 (a) 0 wt %, (b) 0.25 wt %, (c) 1.0 wt % and (d) 2.0 wt %

Table 5.1 Crystal size, surface area and weight fraction of anatase, rutile and brookite
of Al_2O_3/TiO_2 powders calcined at 400°C for 120 minutes

Al_2O_3/TiO_2 (wt %)	Crystallite size (nm)	Surface area (m^2/g)	Amount of Al from ICP (wt %)	W_A	W_R	W_B
0	7.80	80.60	-	0.62	0.19	0.18
0.25	6.90	96.10	0.16	0.70	0.15	0.15
1.0	6.80	99.80	0.83	0.70	0.13	0.17
2.0	6.10	105.70	1.77	0.73	0.12	0.15

W_A : weight fraction of anatase phase

W_R : weight fraction of rutile phase

W_B : weight fraction of brookite phase

That surface is more basic than bare TiO_2, the higher basicity of surface favors dye attachment through its carboxylic acid groups which can cause the increase of absorbed dye amount (Wu et al., 2008, Yang et al., 2009). Therefore, an increase in dye adsorption is expected. Formation of dye agglomerates mainly hinges on to the high acidity nature of the carboxylic groups of the dye or pH of electrolytic composition or surface chemical property of material. The isoelectric point (IEP) of material is the pH at which the materials surface carries no net electrical charge. At a pH below the isoelectric point (IEP), metal oxide surface carries a net positive charge, and above the pH, the negative charge predominates. The isoelectric point (IEP) is therefore an important parameter by which the difference in injection efficiency at the metal oxide|dye interface could also be arisen because it determines the stability of the dye.

Figure 5.2 and Table 5.2 presents the isoelectric point (IEP) values of TiO_2 and Al_2O_3/TiO_2 electrode. It is evident that the isoelectric point (IEP) of all mixing Al_2O_3 electrode are some higher than that of the pure TiO_2 electrode. So when adsorbed with N3, the absorbance of the Al_2O_3/TiO_2 electrode is enhanced compared with that of the TiO_2 electrode, showing that the modification of Al_2O_3 apparently increases the amount of adsorbed dye molecules (show in Figure 5.3). The higher amount of dye molecules is attributed to the higher basicity of the TiO_2 electrode upon Al_2O_3 modification. It has been observed that the carboxyl groups in the N3 dye molecules are more easily adsorbed to the surface of the layers if the modification materials are more basic than TiO_2 (Jung et al., 2005).
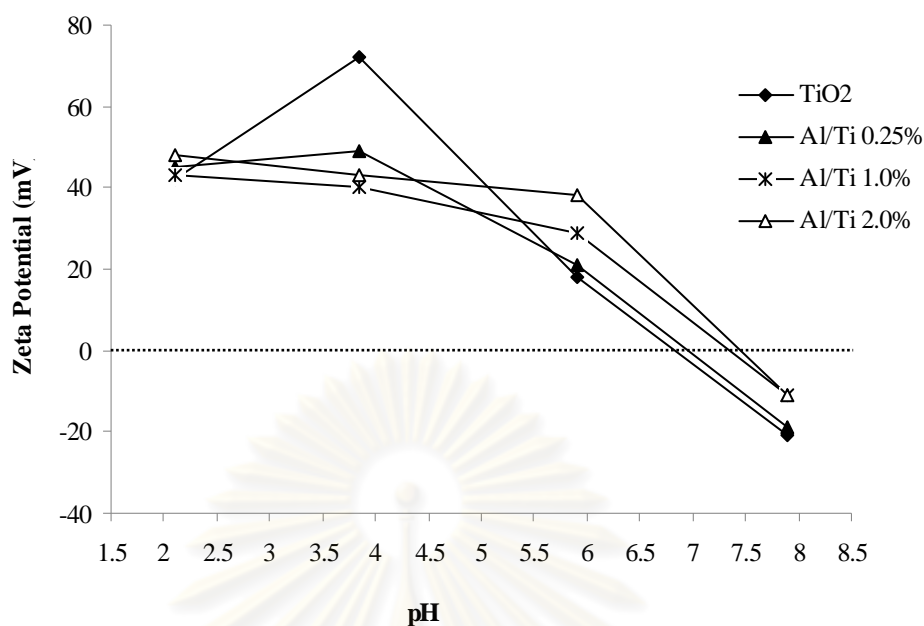
Figure 5.2 Isoelectric point (IEP) of TiO$_2$ modified with various Al$_2$O$_3$ contents

Table 5.2 The isoelectric point (IEP) of TiO$_2$ and Al$_2$O$_3$/TiO$_2$ at various percentage of Al$_2$O$_3$/TiO$_2$

Al$_2$O$_3$/TiO$_2$ (wt %)	Isoelectric point (IEP)
0	6.69
0.25	6.81
1.0	7.20
2.0	7.33

Quantitative analysis was done by desorbed dye molecules from presoaked TiO$_2$ and Al$_2$O$_3$/TiO$_2$ film into a solution of 0.1 M NaOH in ethanol (1:1 in volume fraction) and measuring its absorption spectrum. The amount of the adsorbed dye on TiO$_2$ and Al$_2$O$_3$/TiO$_2$ was also showed in Figure 5.3.

Figure 5.3 shows the UV–visible absorption spectra for N3 dye absorbed TiO$_2$ and Al$_2$O$_3$/TiO$_2$ electrodes. The wavelength of laser was selected as 510 nm because the dye molecules have maximum absorption around this wavelength. It can be

concluded that absorption is enhanced with increasing the contents of Al_2O_3 modification. The increased absorption led to enhanced light harvesting and thereby increased short circuit photocurrent (current density) for the corresponding DSSC. It is assumed that the Al_2O_3/TiO_2 layer can also adsorb the dye, which absorbs the light and generates excited states of the dye.

Figure 5.4 shows the FT-IR spectra of modified TiO_2 with the different of Al_2O_3 contents. The 1600 and 1380 cm^{-1} peaks were attributed to the asymmetric and symmetric stretching vibrations of $-COO^-$ group (Luo et al., 2008), and their intensity increased with mixing Al up to 1 wt %. Table 5.3 shows the amount of functional groups of carboxylic acid, obtained by calculating the area under the graph of the functional groups divided by the surface area. Both UV-vis and FT-IR spectra data support the finding that the carboxylate acid in N3-TiO_2 after Al_2O_3 addition. After adding Al to 2 wt % the results are shown carboxylate acid on the surface decrease and the amount of dye absorption decreased. These results clearly indicate that N3 should also adsorb on TiO_2 powder surfaces via its carboxylate form. Besides, although a large number of the carboxyl groups in the dye sensitizer will increase the electron transfer efficiency due to their better anchoring to the TiO_2 surface (Chen et al., 2010).
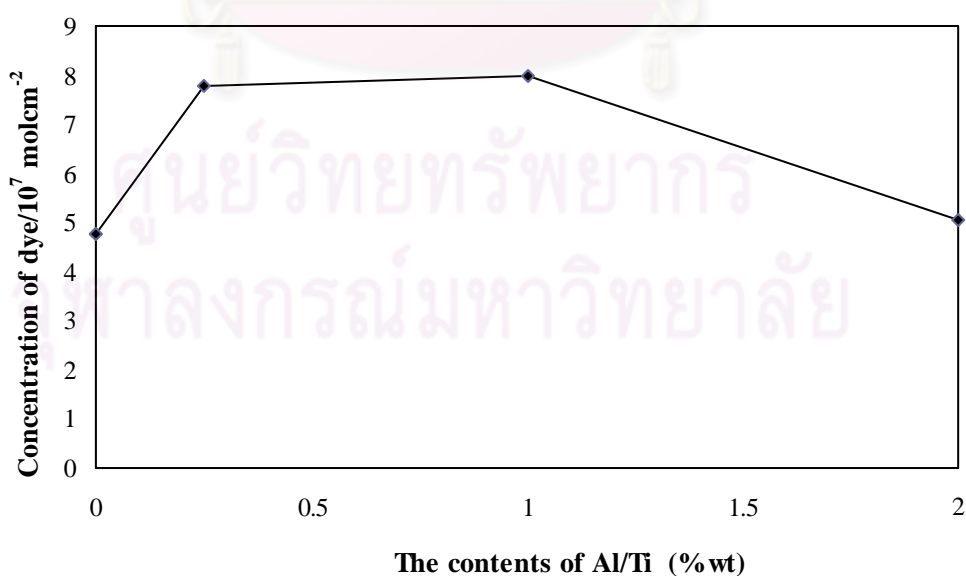
Figure 5.3 Relationship between concentrations of dye with various contents of
Al_2O_3/TiO_2
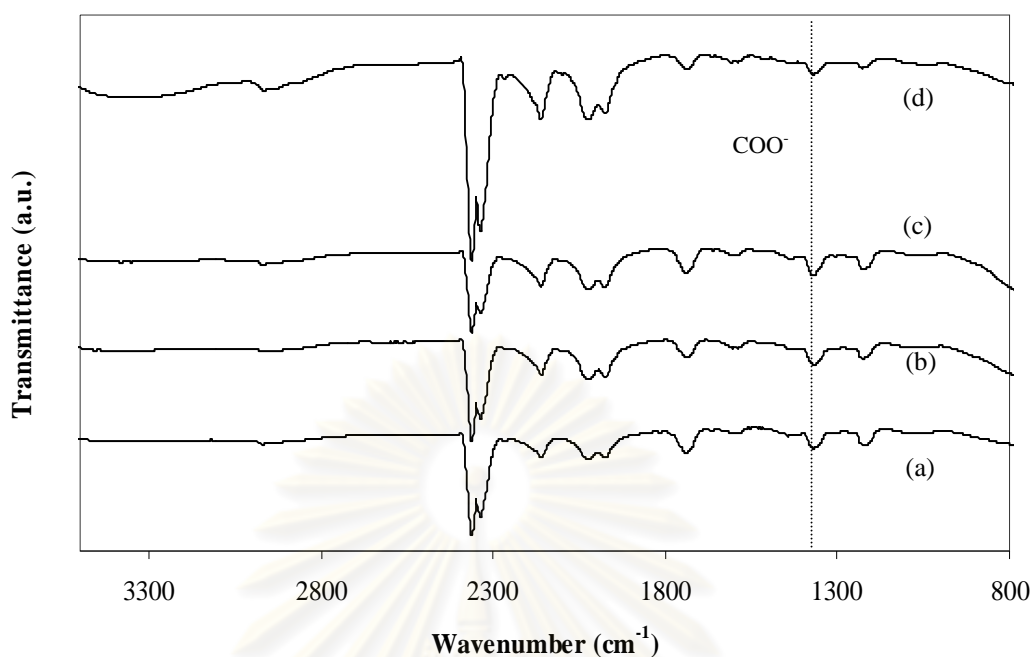
Figure 5.4 FTIR spectra of modified TiO_2 with various Al_2O_3 contents

(a) 0 wt %, (b) 0.25 wt %, (c) 1.0 wt % และ (d) 2.0 wt %

Table 5.3 The quantity of carboxylate acid group on surface of TiO_2 and Al_2O_3/TiO_2
at various percentage of Al/Ti

Al_2O_3/TiO_2 (wt %)	Weight (g)	Surface area (m^2/g)	Area peak of COO^-	Surface area×Weight = Surface total	Area peak of COO^- per Surface total
TiO_2	0.001	80.60	113.78	0.08	1411.70
0.25	0.001	96.10	161.74	0.10	1683.10
1.0	0.001	99.80	173.47	0.99	1738.20
2.0	0.0013	105.70	91.15	0.14	663.30

The overall view of the efficiency of cells fabricated from bare TiO_2 and Al_2O_3/TiO_2 electrodes under 100 mW·cm^{-2}illumination. The corresponding solar cell

parameters are summarized in Table 5.4. When the contents of Al_2O_3 is mixed for less than 2.0 wt % a higher short circuit current, open circuit photo-voltage and conversion efficiency with increased the contents of Al_2O_3 can be observed for the electrodes. The cell showed great improvement in the cell parameters when the contents of Al indicated that 1.0 wt % of Al_2O_3/TiO_2 electrode. The current density increased from 6.89 ± 1.4 to 7.85 ± 0.9 mA·cm^{-2}, and the voltage from 0.60 ± 0.1 to 0.80 ± 0.04 volt. The cell conversion efficiency increased from $3.50\pm0.2\%$ to 5.04 ± 0.2 %, showing the positive role of the Al_2O_3 mixing on TiO_2. When the mixing Al was increased to 2.0 wt %, the amount of the dye adsorbed shows decrease with the increase of Al_2O_3 content, which will result in the decrease of the light harvesting efficiency. Upon further increase of mixing the contents of Al_2O_3, the conversion efficiency drastically decreased along with other cell parameters. From the poor conversion efficiencies, it can be inferred that excessive Al_2O_3 beyond tunneling distance plays a negative role in the photoelectron conversion process (Wu et al., 2008)

Table 5.4 Electrochemical properties of dye sensitized solar cell of Al_2O_3/TiO_2 electrode calcined at 400°C with 500 coats

Al_2O_3/TiO_2 (wt %)	V_{oc} (Volt)	J_{sc} (mA·cm^{-2})	Fill Factor	Efficiency (%)
0	0.60 ± 0.1	6.89 ± 1.4	0.89 ± 0.3	3.50 ± 0.2
0.25	0.73 ± 0.01	7.74 ± 0.3	0.71 ± 0.01	4.01 ± 0.08
1.0	0.80 ± 0.04	7.85 ± 0.9	0.81 ± 0.1	5.04 ± 0.2
2.0	0.76 ± 0.01	4.53 ± 0.4	1.00 ± 0.06	3.45 ± 0.09

5.1.2 Modification of TiO$_2$ electrode layer by adding MgO

TiO$_2$ electrode layer was modified by addition of MgO to TiO$_2$ electrode at the percentage of Mg/Ti was 0.25%, 1.0% and 2.0% (wt %), the electrode calcined at 400°C for 120 minutes.

The phase structure of the films was examined by XRD. Figure 5.5 show the XRD pattern of the bare TiO$_2$ and the MgO/TiO$_2$ composite. The peaks are very sharp implying that the TiO$_2$ films were well crystallized (Bihui et al., 2010). The XRD pattern of the MgO/TiO$_2$ composite is found to be similar as that of bare TiO$_2$. Table 5.5 indicated that the additions of magnesium inhibited the anatase phase increase slightly.

Table 5.5 reported the various contents of Mg on Ti catalyst from ICP analysis. From result of ICP analysis found that the contents of Mg less than the nominal value may because the preparation of mixed oxide sol. Besides, this table showed that the crystallite size and surface area which the MgO/TiO$_2$ had higher surface area than pure TiO$_2$.

Generally, for a given dye, the amount of dye adsorbed on TiO$_2$ and MgO/TiO$_2$ is correlated with the specific area of TiO$_2$ and MgO/TiO$_2$. The amount of the adsorbed dye on TiO$_2$ and MgO/TiO$_2$ was also showed in Figure 5.7. It can be observed that the amount of the adsorbed dye decreases with the increase of the MgO content, while its specific surface area increase compared to that of unmodified TiO$_2$ (see in Table 5.5). So the specific surface area was not mainly responsible for the decrease of the dye adsorption.
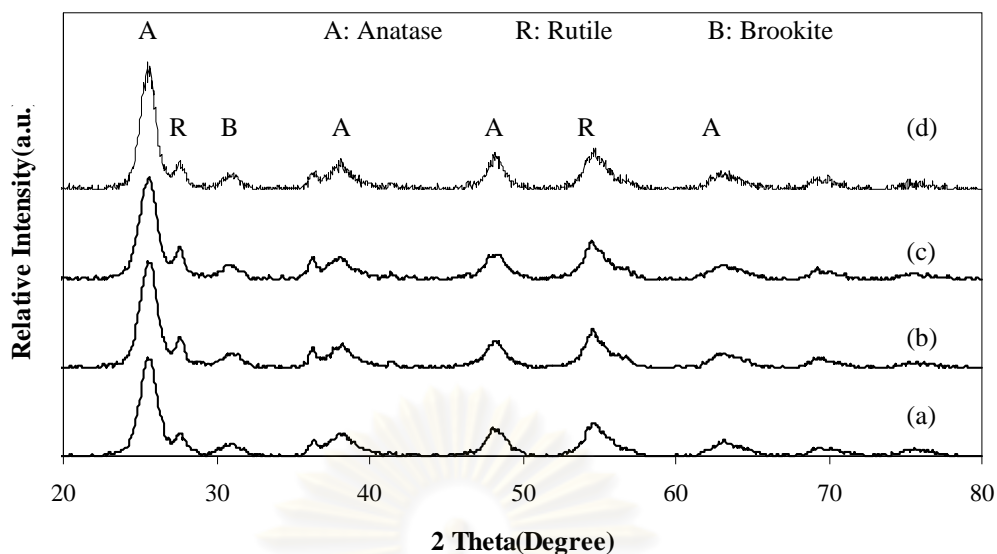
Figure 5.5 XRD patterns of MgO/TiO$_2$ powders at various percentage of Mg/Ti
(a) 0 wt %, (b) 0.25 wt %, (c) 1.0 wt % and (d) 2.0 wt %

Table 5.5 Crystal size, surface area and weight fraction of anatase, rutile and brookite
of MgO/TiO$_2$ powder calcined at 400°C for 120 minutes

MgO/TiO$_2$ (wt %)	Crystallite size (nm)	Surface area (m^2/g)	Amount of Al from ICP (%wt)	W$_A$	W$_R$	W$_B$
0	7.80	80.60	-	0.62	0.19	0.18
0.25	6.40	94.60	0.22	0.70	0.13	0.17
1.0	6.90	90.80	0.42	0.70	0.12	0.17
2.0	7.30	88.50	1.89	0.71	0.13	0.16

In order to clarify the reason that a less dye uptake was obtained for MgO modified TiO$_2$, zeta potentials of the TiO$_2$ particles modified with various MgO contents were measured. Figure 5.6 shows the zeta potential of TiO$_2$ modified with various MgO contents and Table 5.6 presents the isoelectric point (IEP) values of TiO$_2$ and MgO/TiO$_2$ electrode. The results show a clear difference in isoelectric point (IEP) between the samples. It can be clearly observed that the isoelectric point (IEP) of the particles shifts to lower pH values with the increase of MgO content. For a

given curve, when independent variable of pH is less than the isoelectric point (IEP) of TiO_2, the zeta potential for the sample is low the horizontal axis, which means that the surface of MgO/TiO_2 nanopareicles is the higher acidcity of surface, which is adverse to the adsorption of dye molecules onto TiO_2 surface (Cheng et al., 2008). So the isoelectric point (IEP) is responsible for the decrease of the dye adsorption for MgO modified TiO_2.
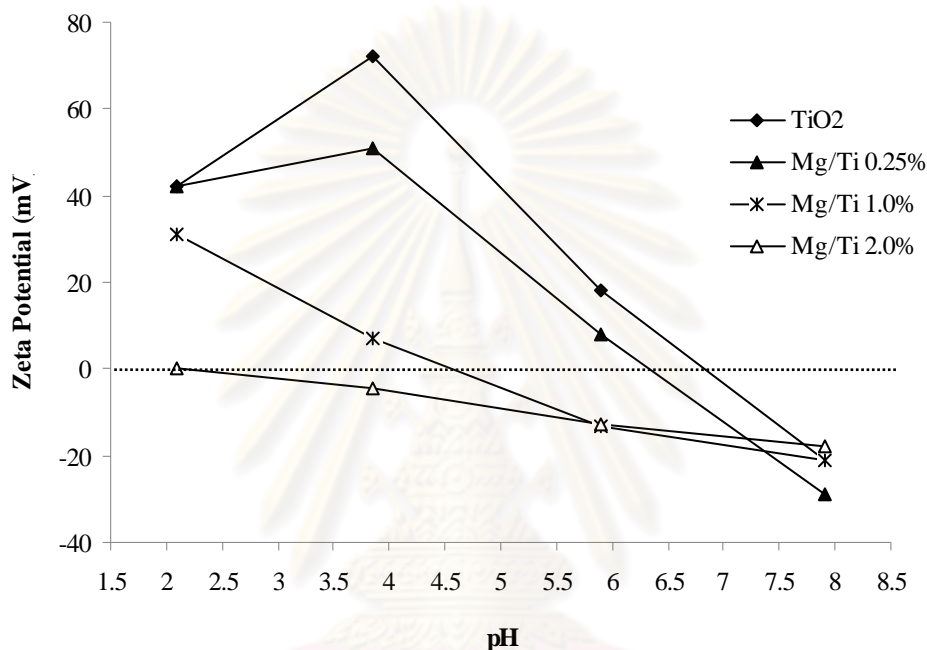
Figure 5.6 Zeta potentials of TiO_2 modified with various MgO contents

Table 5.6 The isoelectric point (IEP) of TiO_2 and MgO/TiO_2 at various percentage of Mg/Ti

MgO/TiO_2 (wt %)	Isoelectric point (IEP)
0	6.69
0.25	6.30
1.0	4.55
2.0	0.63
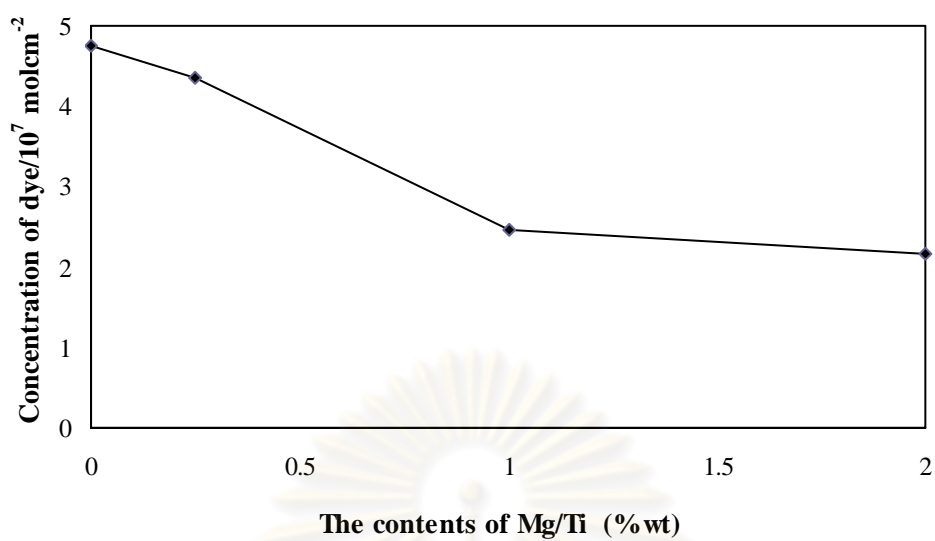
Figure 5.7 Relationship between concentrations of dye with various contents of
MgO/TiO$_2$
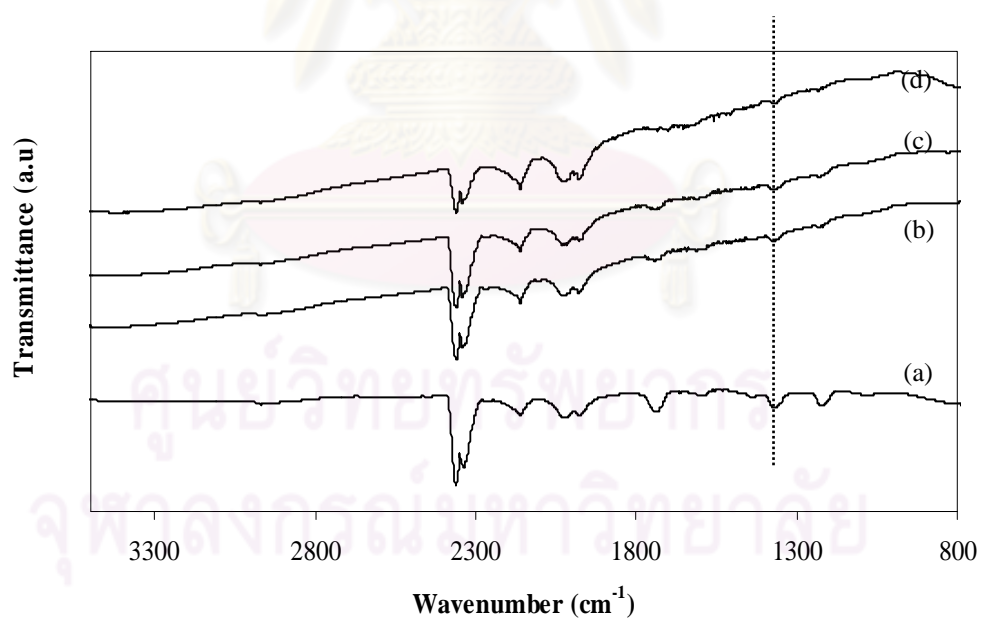
Figure 5.8 FTIR spectra of modified TiO$_2$ with various MgO contents
(a) 0 wt %, (b) 0.25 wt %, (c) 1.0 wt % and (d) 2.0 wt %

If considered carboxylate acid on the surface of TiO_2 after improve. FT-IR results showed that the position wavenumber 1380 cm^{-1} was attributed to the symmetric stretching vibrations of $-COO^-$ group was decreased when the amount of Mg increased. This means that among the adhesive surface is less. Consistent with the results of dye absorption (show in Figure 5.7 and Table 5.7), the amount of dye absorption is reduced. This is because the carboxylic acid group in the dye reacted more favourably on a surface with a more basic nature or higher the isoelectric point (IEP), as show in Table 5.6 (Ganapathy et al., 2010).

The photovoltaic parameters of DSSC of MgO/TiO_2 electrode calcined at 400°C at various the amount of Mg are summarized in Table 5.8. The inset shows the corresponding photocurrent density (J_{SC}) of DSSC. The photocurrent density decreases as a function of MgO content, which confirmed the previous discussion about the dye adsorption effect of MgO modification. So, the overall efficiency of cell was decease after added Mg on Ti sol.

Table 5.7 The quantity of Carboxylate acid group on surface of TiO_2 and MgO/TiO_2 at various percentage of MgO

MgO/TiO_2 (wt %)	Weight (g)	Surface area (m^2/g)	Area peak of COO^-	Surface area×Weight = Surface total	Area peak of COO^- per Surface total
TiO_2	0.001	80.60	113.78	0.08	1411.70
0.25	0.002	94.60	111.97	0.19	591.83
1.0	0.0016	90.80	76.73	0.15	528.06
2.0	0.0013	88.50	64.80	0.12	563.21

Table 5.8 Electrochemical properties of dye sensitized solar cell of MgO/TiO$_2$
electrode calcined at 400°C with 500 coats

MgO/TiO$_2$ (wt %)	V$_{oc}$ (Volt)	J$_{sc}$ (mA·cm^{-2})	Fill Factor	Efficiency (%)
0	0.60±0.1	6.89±1.4	0.89±0.3	3.50±0.2
0.25	0.77±0.06	4.90±0.8	0.75±0.1	2.79±0.07
1.0	0.74±0.02	3.79±0.6	0.82±0.1	2.27±0.09
2.0	0.60±0.04	1.32±0.2	0.52±0.05	0.41±0.05

5.2 Effect of calcinations temperature on mixed oxide electrode layer

Al$_2$O$_3$/TiO$_2$ (1.0 wt %) sol was prepared via sol-gel method. It has been used as a working electrode in DSSC. In general, sintering temperature affect on photocurrent-voltage characteristic because of the change of crystallite size, surface area and phase transformation of TiO$_2$ (Ngamsinlapasathian et al., 2005). In this study, the sintering temperature was varied to be 300°C, 400°C and 500°C.

The crystalline nature of the TiO$_2$ particles was investigated using XRD and the results are shown in Figure 5.9. X-ray diffraction analyses show the presence of anatase structure al low temperature. Fraction of rutile phase is detected with increasing the calcinations temperature 500°C.

Crystalline size of the particles was estimated from the full width at half maximum (FWHM) of the intense (1 0 1) diffraction peak of anatase phase according to the Scherrer's equation. The primary particle sizes of TiO$_2$ particle using Scherrer's equation are listed in Table 5.9. The estimated sizes were 5.2 nm, 7.0 nm and 8.2 nm for sintered temperature at 300°C, 400°C and 500°C, respectively. When the higher temperature, the smaller the BET surface area of the sample. It was also found that the

crystalline size, surface area and phase transformation were affected by the calcinations temperatures.

The increasing of particle size can be attributed of crystallization of the surface amorphous structure and the connection of those small nanoparticles at higher calcined temperature are important for help electron transport of TiO_2 film electrode (Zhao et al., 2008).

Han et al., 2005 have reported that a DSSC with 71% anatase (and remaining rutile) in its film has shown a larger conversion efficiency of 6.8% compared to 5.3% of a cell with pure anatase TiO_2. Conpared with anatase, rutile TiO_2 has superios light scattering properties because of its higher refraction index and is chemically more stable and potentrally cheaper to produce. Higher light scattering properties are beneficial from the perspectives of effective light harvesting.
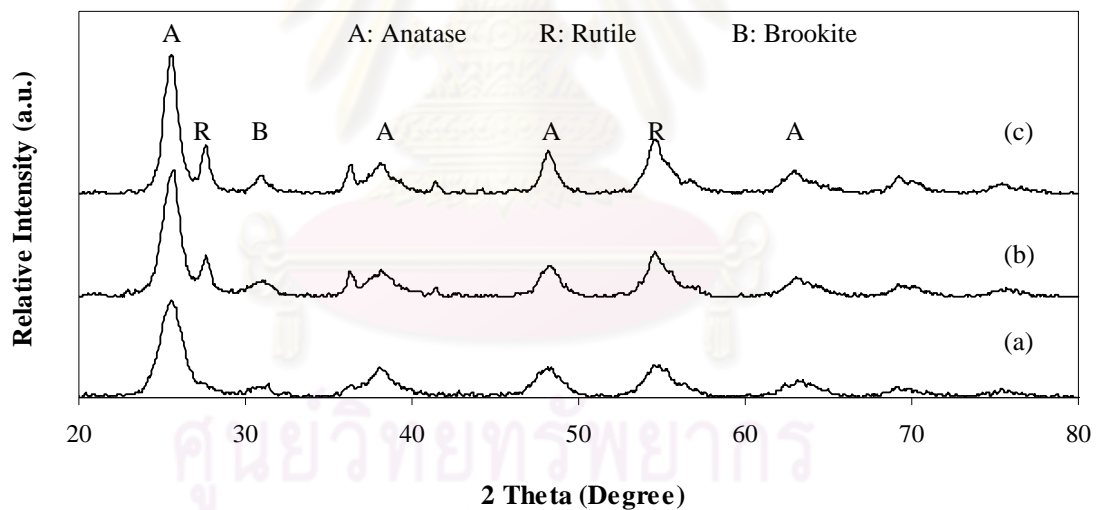
Figure 5.9 XRD patterns of 1.0% (wt %) of Al_2O_3/TiO_2 powders sintered at different temperature for 120 minutes, (a) 300°C, (b) 400°C and (c) 500°C

Table 5.9 Crystal size, surface area and weight fraction of anatase and rutile phase of
1.0 wt % of Al_2O_3/TiO_2 powders at different temperature for 120 minutes

Calcined temperature of 1.0 wt % (°C)	Crystallite size (nm)	Surface area (m²/g)	W_A	W_R	W_B
300	5.20	134.40	0.85	0.04	0.1
400	7.00	99.20	0.70	0.13	0.17
500	8.20	66.90	0.66	0.20	0.14

W_A : weight fraction of anatase phase

W_R : weight fraction of rutile phase

W_B : weight fraction of brookite phase
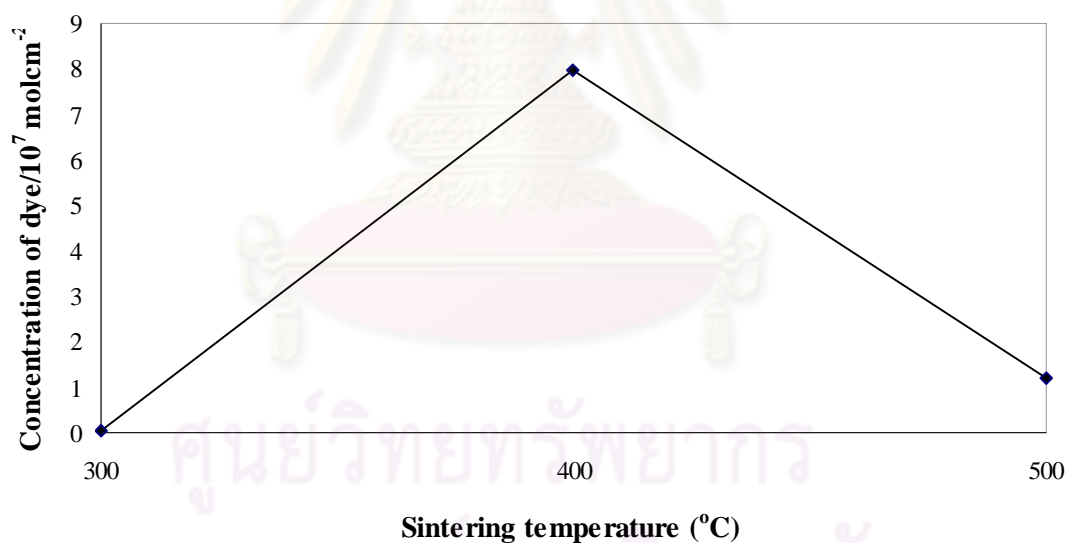
Figure 5.10 Relationship between concentrations of dye and sintering temperatures
with 500 coats of 1.0 wt % of Al_2O_3/TiO_2 for 120 minutes

The resulting of electrochemical properties in Table 5.10 of the thickness of
TiO_2 was about 10.5 µm at various sintering temperature for 120 minutes indicated
that sintering temperature influence on performance of DSSC, this table ware show
short-circuit current (Jsc), open-circuit voltage (Voc), fill factor (FF) and efficiency of
DSSC.

The photocurrent characteristic (Jsc) increases maximal up to 400°C and it decreases with increases in sintering temperature. Although surface area of the cell calcined at 400°C less than the cell calcined at 300°C, in contrast the amount of dye adsorption of electrode sintered at 400°C higher than the electrode sintered at 300°C. In general, the amount of adsorbed dye increases related with number of inject electron in metal electrode leading to an increase of Jsc. Hence, the electrode was calcined at 400°C improve the connection between particles which help electron transport of TiO_2 film electrode.

The efficiency of the cell sintered at 500°C decreases was show Table 5.10 because of the increasing of rutile phase was show in Table 5.9 leading to large particle size, less of surface area which due to absorption of dye not enough. Beside, it is well known that electron diffusion coefficient (Dn) for the rutile film is about one order of magnitude lower than that of the anatase film, implying that electron transport is slower in the rutile layer than in the anatase layer (Park et al., 2010), it cause current density decreases with the performance of dye sensitized decreases.

Table 5.10 Electrochemical properties of dye sensitized solar cell of 1.0 wt % of Al_2O_3/TiO_2 electrode calcined at various temperatures for 120 minutes, the thickness of Al_2O_3/TiO_2 film about 10.5 µm

Sintering temperature of Al_2O_3/TiO_2 (1.0 wt %), (°C)	V_{oc} (Volt)	J_{sc} (mA·cm^{-2})	Fill Factor	Efficiency (%)
300	0.59±0.005	1.90±0.5	0.49±0.07	0.54±0.1
400	0.80±0.04	7.85±0.9	0.81±0.1	5.04±0.2
500	0.74±0.01	5.51±0.3	1.01±0.04	4.16±0.14
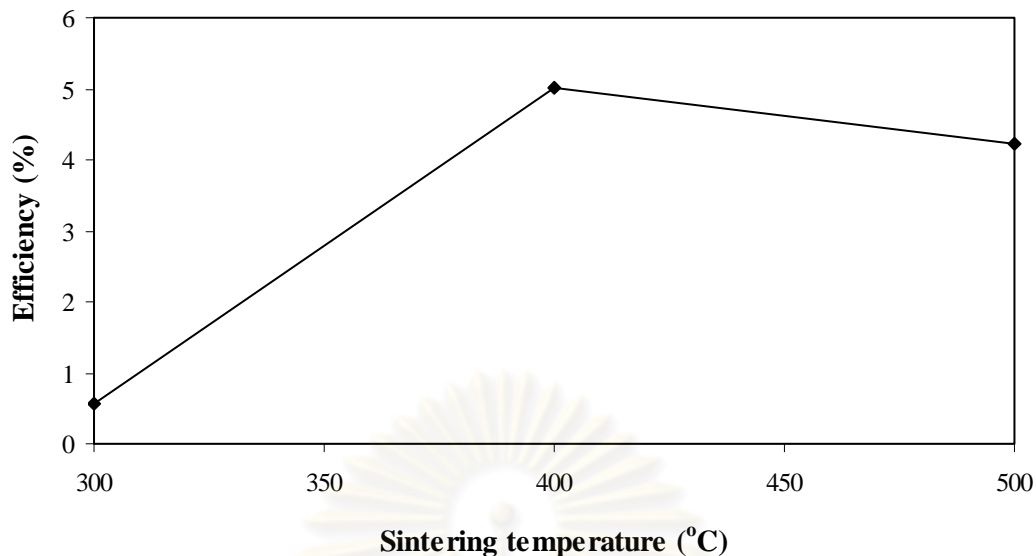
Figure 5.11 The efficiency of 1.0% (wt %) of Al_2O_3/TiO_2 at different calcined temperatures for 120 minutes

5.3 Dye-sensitized solar cell using double-layered conducting glass

TiO_2 electrode was deposited onto conducting glass by the layer-by-layer deposition of double-layered TiO_2 particles. The layer was coated on conducting glasses by using the ultrasonic spray coater, number of coats constant at 500. After deposition, thin film was dried by a hair dryer and then sintered at 400°C. It is expected that the double layer film electrode can be extended to other composite films with different layer structures and morphologies for enhancing the efficiencies of DSSC.

Type A: Deposition Al_2O_3/TiO_2 1.0 wt % sol on a conducting glass, calcined at 400°C for 120 minutes and the number of coats were 500 coats have film thickness was approximately 10.5 µm which sinter temperature, the thickness and the percentage of Al gave highest the efficiency of dye sensitized solar cell.

Type B: Deposition pure TiO_2 sol on a conducting glass and the number of coats were 250 coats and then sintered at 400°C for 120 minutes. Next, the deposition process of the mixed oxide electrode Al_2O_3/TiO_2 1.0 wt % was to obtain the desired

film thickness same single-layer electrode. The electrode was finally sintered at a temperature 400°C for 30 minutes.

After the above heat treatment procedure, the resulting TiO_2 electrodes were soaked in an ethanol solution containing 0.5mM N3 dye at room temperature for 12 hour. Then the electrodes were sequentially washed with ethanol and dried. In order to analyze the loading amount of dye in TiO_2 electrode, the dye was desorbed from TiO_2 electrode into NaOH solution in ethanol. The UV-vis spectrophotometer was employed to measure the dye concentration of the desorbed dye solution. The UV-vis spectrum showing the adsorbent of wavelength for TiO_2 electrode can be observed to have the absorption feature. Table 5.11 shows the comparison of concentration of dye value between a single layered and double layered electrode structure. The adsorption of dye in single layered and double layered are 7.9725×10^{-7} mol·cm^{-2} and 8.5048×10^{-7} mol·cm^{-2}, respectively. Consequently, it can be confirmed that the conjugation status exists between dye and the thin film electrode, and multiple layered organization will affect photoelectrical electrode production. When compared with single layered and double layer thin film result the prepared double layer thin film with a good compactness can increase the dye adsorption capability of the thin film and enhance its adsorption percentage. These dyes should incorporate functional groups (interlocking groups) as for example carboxylates or chelating groups, which besides bonding to the titanium dioxide surface, also effect an enhanced electronic coupling of the sensitizer with the conduction band of the semiconductor. The carboxylates groups serve to attach the Ru complex to the surface of the oxide and to establish good electronic coupling between the π^* orbital of the electronically excited complex (Gratzel et al., 2003, Nazeeruddin et al., 1993).

	Al/Ti 1.0 wt % at 400°C for 30 min
Al/Ti 1.0 wt % at 400°C for 2 hr	Pure TiO$_2$ at 400°C for 2 hr
Conducting glass	Conducting glass

(a)   (b)
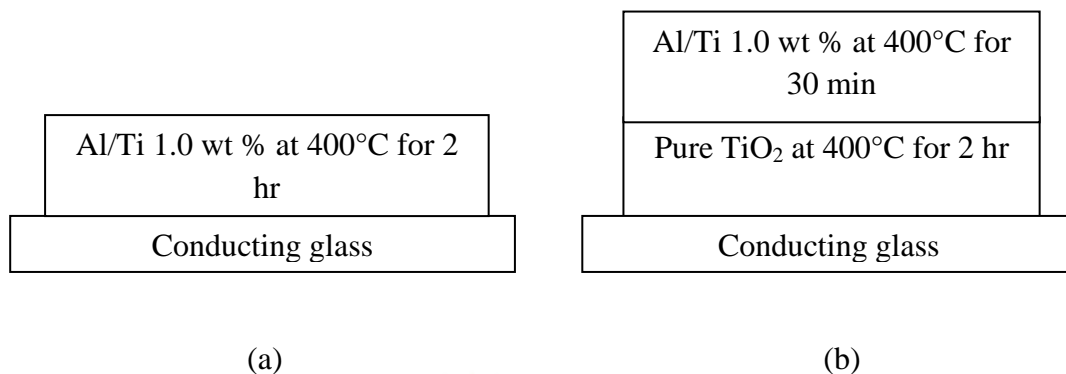
Figure 5.12 Type of the mixed oxide electrode on conducting glass prepared for DSSC (a) Single-layer and (b) Double-layers

Table 5.11 The specific surface area of TiO$_2$ powders calcined at various temperatures

	Calcined temperature (°C)	Crystallite size (nm)	Surface area (m^2/g)	Concentration of dye (mol·cm^{-2})
Single-layer :				
Al$_2$O$_3$/TiO$_2$ 1.0 wt %	400°C 120 min	6.95	99.20	7.97×10^{-7}
Double-layers :				
Pure TiO$_2$ (underlayer)	400°C 120 min	7.80	80.60	8.50×10^{-7}
Al$_2$O$_3$/TiO$_2$ 1.0 wt % (overlayer)	400°C 30 min	5.69	120.20	

      Figure 5.13 represents the diffused reflection spectra of single-layered and double-layer TiO$_2$ electrode. The diffused reflectance of the films increases as the scattering layers were added.

      Table 5.12 compared the properties and photovoltaic parameters of single layered and double layered thin film electrode at nearly specific surface area, in which the thickness of single-layered electrode was experimentally controlled to be identical to that of double-layered electrode (ca. 10.5µm). As a result, from many dye

molecules are adsorbed on the surface of modification TiO_2 film structure, increases the photocurrent value (J_{SC}) from 7.85±0.9 to 8.74±0.9 mA·cm^{-2} and the photoelectrochemical properties of the double layer structure were improved and the overall energy conversion efficiency η was enhanced from 5.04±0.2% to 5.50±0.5%.
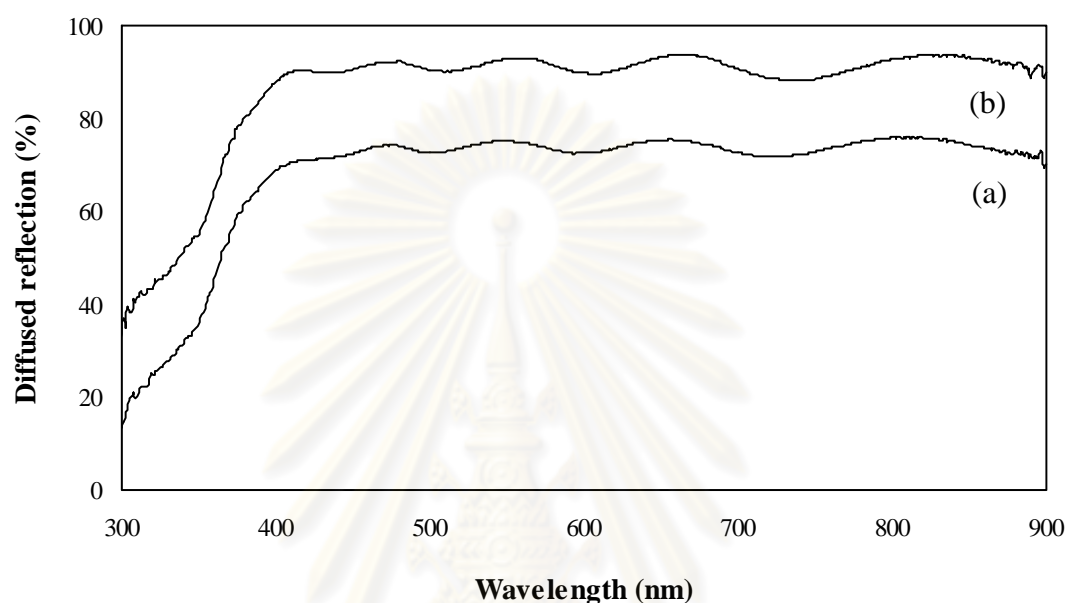
Figure 5.13 Diffused reflection of single-layered and double-layered

(a) Single-layer and (b) Double-layer

Table 5.12 DSSC performance of single and double layers electrode

	V_{oc} (volt)	J_{sc} (mA·cm^{-2})	Fill Factor	Efficiency (%)
Single-layer :				
Al_2O_3/TiO_2 1.0 wt %	0.80±0.04	7.85±0.9	0.81±0.1	5.04±0.2
Double-layers :				
Pure TiO_2 (under)				
Al_2O_3/TiO_2 1.0 wt % (over)	0.73±0.005	8.74±0.9	0.86±0.03	5.50±0.5

CHAPTER VI
CONCLUSIONS AND RECOMMENDATIONS

FOR FUTURE RESEARCH

This research has investigated the effect of TiO_2 with the addition of alumina or magnesium oxide on the performance of dye-sensitized solar cell. In this chapter, section 6.1 provided the conclusion that obtained from the experimental results of the effect of the modification of TiO_2 electrode layer by adding Al_2O_3 and MgO, the effect of sintering temperature, effect of thickness of TiO_2 electrode layer for single-layer and double-layer TiO_2 films on the performance of dye-sensitized solar cell. Additionally, recommendations for future study are presented in section 6.2.

6.1 Conclusion

6.1.1 Modification of TiO_2 electrode layer by adding Al_2O_3

The modification of the TiO_2 electrode layer by different amount of Al_2O_3 by weight altered the performance of dye-sensitized solar cell. The surface area of TiO_2 after the addition of alumina also has a lot more basicity. Resulting dye molecules (with a group carboxylate acid) adhesive on the surface more. Lead to improved short circuit current density and the efficiency of the cells when compared to cells with only TiO_2. The 1% (wt %) of Al_2O_3/TiO_2 electrode sintered at 400 °C for two hours at thickness of film was 10.5 μm gave the best efficiency of cell of 5.04±0.2%.

6.1.2 Modification of TiO_2 electrode layer by adding MgO

The effect of adding magnesium oxide the surface of titanium dioxide after the addition the acidity increased. The amount of dye absorption decreased, resulting in reduced short circuit current density and efficiency of the cell decreased when compared to cells with only TiO_2.

6.1.3 Effect of sintering temperature on mixed oxide electrode layer

The photovoltaic parameters of DSSC depend on sintering temperature, it was found that a maximum of short-circuit current density with a DSSC with a TiO_2 added alumina 1% (wt %) electrode sintered at 400°C for 120 minutes. The highest cell efficiency of $5.04\pm0.2\%$.

6.1.4 Double-layered TiO_2 electrode

Double-layered TiO_2 electrode was fabricated to increase the light scattering and dye adsorption. The photoelectrochemical properties of the double layer structure were improved and the overall energy conversion efficiency was enhanced from $5.04\pm0.2\%$ to $5.50\pm0.5\%$.

6.2 Recommendations for future studies

From the previous conclusions, the following recommendations for future studies are proposed.

1. Improving efficiency of dye-sensitized solar cell by optimizing fabrication procedure.
2. Improving of the light harvest efficiency of dye-adsorbed TiO_2 electrodes by multi-layer (using a TiO_2 layer higher surface area increases the dye adsorption).
3. Improving the surface of TiO_2 electrode with other metal oxide.

REFERENCES

Bandara, J., and Pradeep, U.W. Tuning of the flat-band potentials of nanocrystalline TiO_2 and SnO_2 particles with an outer-shell MgO layer. Thin Solid Films 517 (2008): 952-956.

Bihui, L., Gang, L., Lijuan, L., and Yiwen, T. TiO_2@MgO core-shell film: Fabrication and Application to Dye-sensitized solar cells. Journal of Natural Sciences (2010): 325-329.

Chen, G., Zheng, K., Mo, X., Sun, D., Meng, Q. and Chen, G. Metal-free indoline dye sensitized zinc oxide nanowires solar cell. Journal of Materials Letters 64 (2010): 1336-1339.

Cheng, P., Deng, C., Dai, X., Li, B., Liu, D. and Xu, J. Enhanced energy conversion efficiency of TiO_2 electrode modified with WO_3 in dye-sensitized solar cells. Journal of Photochemistry and Photobiology A: Chemistry 195 (2008): 144-150.

César, O., Avellaneda, Agnaldo, D. Gonçalves,. João, E., Benedetti, and Nogueira, F. Preparation and characterization of core-shell electrodes for application in gel electrolyte-based dye-sensitized solar cells. Journal of Electrochimica Acta 55 (2010): 1468-1474.

Gratzel, M. Dye-sensitized solar cells: review. Journal of Photochem. Photobiol. C: Rev. 4 (2003): 145-153.

Green, M.A., Enery, K., Hisikawa, Y., Warta, W. and Prog. PhotovoHaics 15 (2007): 425-430.

Ganapathy, V., Karunagaran, B. and Shi-Woo Rhee. Improved performance of dye-sensitized solar cells with TiO_2/alumina core-shell formation using atomic layer deposition. Journal of Power Sources 195 (2010): 5138-5143.

Gregg, B.A., Pichot. F., Ferrere, S. and Fields, C.L. Journal of Physics and Chemisty: B 105 (2001): 1422-1429.

Hsiue-Hsyan, W. Preparation of Nanoporous TiO$_2$ Electrode for DSSC (2010)

Han, H., and Zhao, J. Enhancement in photoelectric conversion properties of the dye-sensitized nanocrystalline solar cell based on the hybride TiO$_2$ electrode. Journal of the Electrochemical Society 152 (2005) A164-A166.

Harizanov, O., and Harizanova, A. Solar Energy Materials & Solar Cells 63 (2000): 185-195.

Jung, H., Lee, J. and Nastasi, M. Langmuir (2005): 10332-10335.

Kalyanasundaram, K. and Grätzal, M. Application of functionalized transition metal complexes in photonic and optoelectronic devices. Journal Coordination Chemistry Reviews 77 (1998): 347-414.

Katoh, R., Akihiro, F., Alexander, V., Hironori, A., and Tachiya, M. Kinetics and mechanism of electron injection and charge recombination in dye-sensitized manocrystalline semiconductors. Journal of Coordination Chemistry Reviews 248 (2004): 1195-1213.

Ko, K.H., Lee, Y.C. and Jung, Y.J. Enhanced efficiency of dye-sensitized TiO$_2$ solar cells (DSSC) by doping of metal ions. Journal of Colloid Interface 283 (2005): 482-487.

Lee, S. and others. Preparation of a nanoporous CaCO$_3$-coated TiO$_2$ electrode and its application to a dye-sensitized solar cell. Langmuir 23 (2007): 11907-11910.

Lee, J. and others. Preparation of TiO2 pastes and its application to light-scattering layer for dye-sensitized solar cells. Journal of Industrial and Engineering Chemistry 15 (2009): 724-729.

Liu, Z. and others Electrochim. Acta 50 (2005): 2583-2589.

Lou, F., Liduo, W., Beibei, M., and Yong, Q. Post-modification using aluminum isopropoxide after dye-sensitization for improved performance and stability of quasi-solid-state solar cells. Journal of Photochemistry and Photobiology 197 (2008): 375-381.

Mathews, N.R., Morales, R., Cortés-Jacome, M.A. and Toledo Antonio, J.A. TiO$_2$ thin films-Influence of annealing temperature on structural, optical and photocatalytic propertics. Journal of Solar Energy 83 (2009): 1499-1508.

Mishra, P.R., Shukla, P.K., Singh, A.K. and Srivastava, O.N. Investigation and optimization of nanostructured TiO$_2$ photoelectrode in regard to hydrogen production through photoelectrochemical process. Journal of Hydrogen Energy 28 (10)(2003): 1089-1094.

Nazeeruddin, M.K., Kay, A. and Gratzel, M. Conversion of light to electricity by cis-X2bis (2,2'-bipyridyl-4,4'-dicarboxylate)ruthenium (II) charge-transfer sensitizers (X=Cl-, Br-, I-, CN-, and SCN-) on nanocrystalline titanium dioxide electrodes. . Journal of American Chemical Society 115 (1993) 6382-6390.

Nazeeruddin, M.K., Humphry-Baker, R., Liska, P. and Graetzel, M., Journal of Physics and Chemisty B 107 (2003): 8981-8987.

Nilsing, M., Persson, P., Lunell, S. and Ojamaee, L., Journal of Physics and Chemisty C 111 (2007): 12116-12123.

Ngamsinlapasathian, S., Sreethawong, T., Suzuki, Y., and Yoshikawa, S. Single- and double-layered mesoporous TiO$_2$/P25 TiO$_2$ electrode for dye sensitized solar cell. Solar Energy Materials & Solar Cells 86 (2005): 269-282.

Oregen, B., and Grätzel, M. A low-cost high efficiency solar cell based on dye-sensitized colloidal TiO$_2$ film. Nature 353 (1991): 737-740.

Rochfoed, J., Chu, D., Hagfeldt, A. and Galoppini, E. Journal of American Chemical Society 129 (2007): 4655-4665.

Thavasi, V., Renugopalakarishnan, V., Juse, R. and Ramakrishna, S. Journal of Materials Science and Engineering R63 (2009): 81-99.

Takikawa, H., Matsui, T., Sakakibara, T., Bendavid, A. and Martin, P.J. Properties of titanium oxide film prepared by reactive cathodic vacuum are deposition. Thin Solid Films 348 (1999): 145-151.

Wu, S. and others. Improvement in dye-sensitized solar cells employing TiO_2 electrodes coated with Al_2O_3 by reactive direct current magnetron sputtering. Journal of Power Sources 182 (2008): 119-123.

Xia, J., Masaki, N., Jiang, K. and Yanagida, S. Sputtered Nb_2O_5 as a novel blocking layer at conducing glass/TiO_2 interfaces in dye-sensitized ionic liquid solar cell. Journal of Physical Chemistry C 111 (2007): 8092-8097.

Xu, H., Tao, X., Wang, D., Zheng, Y. and Chen, J. Enhanced efficiency in dye-sensitized solar cells based on TiO_2 nanocrystal/nanotube double-layered films. Journal of Electrochimica Acta (2009).

Yang, S.M., Huang, O.H. and Zhao, X.S. Enhanced energy conversion efficiency of the Sr^{2+}-modified nanoporous TiO_2 electrode sensitized with a ruthenium complex. Chem. Mater. 14 (2002): 1500-1504.

Yu, J., Zhao, X. and Zhao, Q. Photocatalytic activity of nanometer TiO_2 thin films prepared by the sol-gel method. Journal of Materials Chemistry and Physics 69 (2001): 25-29.

Yung, S., Kou, H., Song, S., Wang, H. and Fu, W. Eng-Aspects. 340 (2009): 182-186.

Zhao, D., Peng, T., Lu, L., Cai, P., Jiang, P., and Bian, Z. Effect of annealing temperature on the photoelectrochemical properties of dye sensitized solar cells made with mesoporous TiO_2 nanoparticles. Journal of Physical chemistry C 112 (2008): 8486-8494.

APPENDICES

APPENDIX A

CALCULATION OF THE CRYSTALLITE SIZE

Calculation of the crystalline size by Debye-Scherrer equation

The crystalline size can be calculated from the width at half-height of the diffraction peak of XRD pattern using the Debye-Scherrer equation

From Scherrer equation

$$D = \frac{k\lambda}{\beta\cos\theta}$$
(A. 1)

where   D = Crystallite size, Å

               K = Crystalline-shape factor = 0.9

               λ = X-ray wavelength, 1.5418 Å for CuKα

               θ = Observed peak angle, degree

               β = X-ray diffraction broadening, radian

The X-ray diffraction broadening (β) is the pure width of the powder diffraction, free of all broadening due to the experimental equipment. Standard α-alumina is used to observe the instrumental broadening since its crystallite size is larger than 2000Å. The X-ray diffraction broadening (β) can be obtained by using Warren's formula.

From Warren's formular:

$$\beta^2 = B_M^2 - B_S^2 \qquad\qquad (A.\ 2)$$

$$\beta = \sqrt{B_M^2 - B_S^2}$$

Where B_M =   Measured peak width in radians at half peak height

         B_S =   Corresponding width of a standard material

Example: calculation of the crystallite size of TiO_2

The half-height width of (101) diffraction peak   = $1.0659°$

                                                        = 0.018594 radian

The corresponding half-height width of peak of TiO_2 = 0.003836 radian

The pure width   = $\sqrt{B_M^2 - B_S^2}$

                          = $\sqrt{0.018584^2 - 0.003836^2}$

                          = 0.0182 radian

β = 0.0182 radian

2θ = $25.55°$

θ = $12.775°$

λ = $1.5418\ \text{Å}$

The crystalline size   = $\dfrac{0.9 \times 1.5418}{0.0182\cos 12.775}$ = $78.18\ \text{Å}$ = 7.82 nm
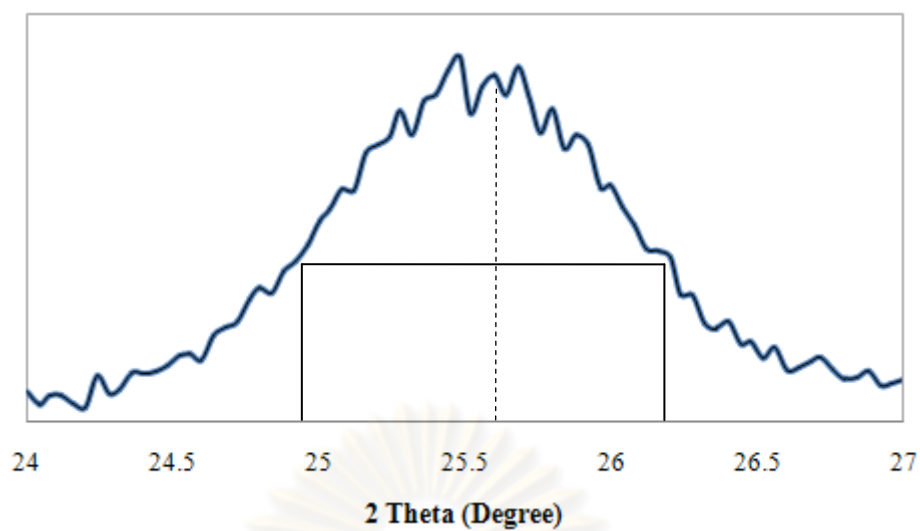
Figure A.1 The (101) diffraction peak of TiO₂ for calculation of the crystallite size

APPENDIX B

CALCULATION OF WEIGHT FRACTION OF ANATASE, RETILE AND BROOKITE PHASE

The phase content of a sable were determined by XRD which can be calculated from the integrated intensities at 2θ values of $25.32°$, $27.44°$, and $30.88°$ corresponded to the anatase, rutile and brookite phase, respectively.

The weight fraction of the phase content can be calculated by (Zhang, Banfield, 2000) as follows:

$$W_A = \frac{k_A A_A}{k_A A_R + A_R + k_B A_B}$$

$$W_A = \frac{A_R}{k_A A_R + A_R + k_B A_B}$$

$$W_B = \frac{k_B A_B}{k_A A_R + A_R + k_B A_B}$$

Where

W_A = weight fraction of anatase

W_R = weight fraction of rutile

W_B = weight fraction of brookite

A_A = the intensity of the anatase peak

A_R = the intensity of the rutile peak

A_B = the intensity of the brookite peak

k_A = the coefficients factor of anatase was 0.886

k_B = the coefficients factor of rutile was 2.721

Example: calculation of the phase contents of TiO_2 calcined 400°C

Where

The integrated intensities of anatase (A_A) = 444.47

The integrated intensities of rutile (A_R) = 122.25

The integrated intensities of brookite (A_B) = 41.83

The weight fraction of the phase content can be calculated by (Zhang, Banfield, 2000) as follows:

$$W_A = \frac{0.886(444.47)}{0.886(444.47) + (122.25) + 2.721(41.83)} = 0.62$$

$$W_A = \frac{122.25}{0.886(444.47) + (122.25) + 2.721(41.83)} = 0.19$$

$$W_A = \frac{2.721(41.83)}{0.886(444.47) + (122.25) + 2.721(41.83)} = 0.18$$

APPENDIX C

DETERMINATION OF THE AMOUNT OF DYE ADSORBED ON TITANIA SURFACE

The amount of dye adsorbed was determined by UV-Visible Absorption Spectroscopy (UV-Vis) where measuring the concentration of dye desorbed on the titania film into a mixed solution of 0.1M NaOH and ethanol (1:1 in volume fraction).

The calibration curve of the concentration of dye with absorbance was illustrated in the following figure.
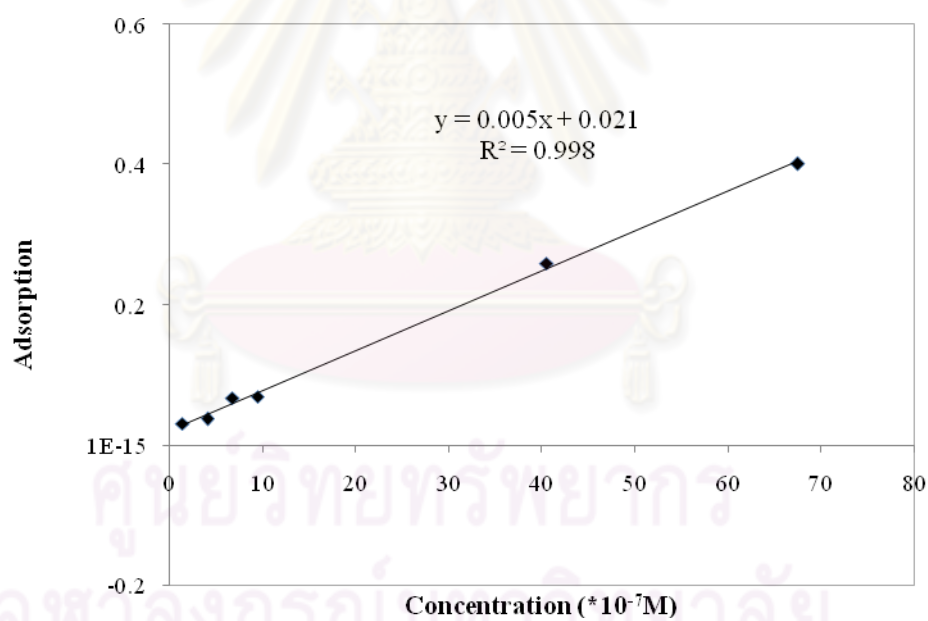
Figure C.1 The calibration curve of the concentration of dye adsorbed

APPENDIX D

CALCULATION OF RESULT OF ICP-OES

Calculation of ICP-OES results

The results from ICP-OES characterization were calculation the contents of metal in catalysts. The example of calculation is as following:

Example: calculation of the contents of 1.0 wt % of Al/Ti in Al_2O_3/TiO_2 powder.

For 1.0 wt % of Al/Ti powder, the initial weight of powder was 0.0126 g.

Hence, the calculation of the alumina contents the catalysts as follows:

The amounts of alumina in the catalyst were;

In 100 g of the Al_2O_3/TiO_2, had a alumina content was   1.0 %

In 0.0126 g of the Al_2O_3/TiO_2, had a alumina content was $\dfrac{0.0173 \times 1.0}{100}$

$$= \ 0.126 \ mg$$

For digest a samples were diluted to 10 cm^3 of volume

Therefore;

The sample had a concentration were $= \ \dfrac{0.126 \times 1000}{10} \ = \ 12.6 \ ppm$

From the result of ICP-OES, shown the contents of alumina was 10.46   ppm

Therefore;

The alumina contents in the catalysts were calculated by

The alumina concentrations were 12.6 ppm refer 1.0 wt % of alumina in catalyst.

The alumina concentrations were 10.46 ppm refer $\dfrac{10.46 \times 1.0}{12.6}$

$$= 0.83 \text{ wt \% of alumina in the catalyst}$$

APPENDIX E

THE ELECTROCHEMICAL PROPERTIES
OF DYE SENSITIZED SOLAR CELL

The electrochemical properties of dye sensitized solar cell as a file thickness and sintering temperature of TiO_2 electrode by I-V tester. In this study three samples were used, and the efficiency of cell given is the average value follow by the standard derivation.

Table E.1 Electrochemical properties of dye sensitized solar cell of TiO_2 electrode calcined at 400°C for 120 minutes, the thickness of TiO_2 film about 10.5 μm

Number of cell	V_{oc} (Volt)	J_{sc} (mA·cm^{-2})	Fill Factor	Efficiency (%)
1	0.51	5.29	1.27	3.40
2	0.65	7.43	0.70	3.36
3	0.68	7.95	0.69	3.74
Average	0.61±0.1	6.89±1.4	0.89±0.3	3.50±0.2

Table E.2 Electrochemical properties of dye sensitized solar cell of 0.25 wt % of
Al$_2$O$_3$/TiO$_2$ electrode calcined at 400°C for 120 minutes, the thickness of
TiO$_2$ film about 10.5 µm

Number of cell	V_{oc} (Volt)	J_{sc} (mA·cm^{-2})	Fill Factor	Efficiency (%)
1	0.74	7.39	0.71	3.92
2	0.73	8.03	0.70	4.07
3	0.73	7.82	0.71	4.03
Average	0.73±0.006	7.74±0.3	0.71±0.005	4.01±0.08

Table E.3 Electrochemical properties of dye sensitized solar cell of 1.0 wt % of
Al$_2$O$_3$/TiO$_2$ electrode calcined at 400°C for 120 minutes, the thickness of
TiO$_2$ film about 10.5 µm

Number of cell	V_{oc} (Volt)	J_{sc} (mA·cm^{-2})	Fill Factor	Efficiency (%)
1	0.82	7.10	0.90	5.28
2	0.75	8.93	0.72	4.83
3	0.83	7.52	0.81	5.02
Average	0.80±0.04	7.85±0.9	0.81±0.1	5.04±0.2

Table E.4 Electrochemical properties of dye sensitized solar cell of 2.0 wt % of
Al_2O_3/TiO_2 electrode calcined at 400°C for 120 minutes, the thickness of
TiO_2 film about 10.5 µm

Number of cell	V_{oc} (Volt)	J_{sc} (mA·cm^{-2})	Fill Factor	Efficiency (%)
1	0.77	4.11	1.06	3.37
2	0.76	4.80	0.94	3.42
3	0.75	4.67	1.01	3.55
Average	0.76±0.01	4.53±0.4	1.00±0.06	3.45±0.09

Table E.5 Electrochemical properties of dye sensitized solar cell of 0.25 wt % of
MgO/TiO_2 electrode calcined at 400°C for 120 minutes, the thickness of
TiO_2 film about 10.5 µm

Number of cell	V_{oc} (Volt)	J_{sc} (mA·cm^{-2})	Fill Factor	Efficiency (%)
1	0.78	4.46	0.81	2.81
2	0.77	5.81	0.61	2.72
3	0.77	4.43	0.83	2.86
Average	0.77±0.06	4.90±0.8	0.75±0.1	2.79±0.07

Table E.6 Electrochemical properties of dye sensitized solar cell of 1.0 wt % of MgO/TiO$_2$ electrode calcined at 400°C for 120 minutes, the thickness of TiO$_2$ film about 10.5 µm

Number of cell	V_{oc} (Volt)	J_{sc} (mA·cm^{-2})	Fill Factor	Efficiency (%)
1	0.71	3.42	0.93	2.25
2	0.76	3.44	0.84	2.19
3	0.74	4.53	0.70	2.38
Average	0.74±0.02	3.79±0.6	0.82±0.1	2.27±0.09

Table E.7 Electrochemical properties of dye sensitized solar cell of 2.0 wt % of MgO/TiO$_2$ electrode calcined at 400°C for 120 minutes, the thickness of TiO$_2$ film about 10.5 µm

Number of cell	V_{oc} (Volt)	J_{sc} (mA·cm^{-2})	Fill Factor	Efficiency (%)
1	0.56	1.41	0.47	0.37
2	0.64	1.05	0.58	0.39
3	0.60	1.49	0.51	0.46
Average	0.60±0.04	1.32±0.2	0.52±0.05	0.41±0.05

Table E.8 Electrochemical properties of dye sensitized solar cell of double-layers
electrode the thickness of Al_2O_3/TiO_2 film about 10.5 µm

Number of cell	V_{oc} (Volt)	J_{sc} (mA·cm^{-2})	Fill Factor	Efficiency (%)
1	0.74	7.76	0.89	5.10
2	0.73	8.53	0.82	5.12
3	0.73	8.13	0.86	5.10
4	0.74	9.88	0.84	6.08
5	0.73	9.41	0.88	6.04
Average	0.73±0.005	8.74±0.9	0.86±0.03	5.50±0.5

ศูนย์วิทยทรัพยากร
จุฬาลงกรณ์มหาวิทยาลัย

APPENDIX F

THE CRYSTALLITE SIZE AND SURFACE AREA OF 1.0 wt % Al_2O_3/TiO_2 POWDERS AT DIFFERENT CALCINATION TEMPERATURE AND TIME

Table F.1 Crystal size, surface area of 1.0 wt % of Al_2O_3/TiO_2 powders calcined for 30 minutes

Calcined Temperature (°C)	Calcined Time (minute)	Crystallite size (nm)	Surface area (m^2/g)
300	30	4.53	161.69
400	30	5.69	120.16
500	30	7.59	79.88

Table F.2 Crystal size, surface area of 1.0 wt % of Al_2O_3/TiO_2 powders calcined for 60 minutes

Calcined Temperature (°C)	Calcined Time (minute)	Crystallite size (nm)	Surface area (m^2/g)
300	60	5.12	146.72
400	60	5.95	110.30
500	60	7.37	80.85

Table F.3 Crystal size, surface area of 1.0 wt % of Al_2O_3/TiO_2 powders calcined for 120 minutes

Calcined Temperature (°C)	Calcined Time (minute)	Crystallite size (nm)	Surface area (m^2/g)
300	120	5.20	134.40
400	120	7.00	99.20
500	120	8.20	66.90

VITA

Miss Jeerapa Tammasanit was born on August 21, 1986 in Rayong, Thailand. She finished high school from Sunthonphu pittaya School, Rayong, and received the bachelor's degree of Chemical Engineering, Burapha university, Chonburi. The she continued his master degree in Chemical Engineering at Chulalongkorn University.

Jeerapa Tammasanit and Akawat Sirisuk. Dye-sensitizer solar cell with Al_2O_3/TiO_2 or MgO/TiO_2 composite thin electrode layer. Proceeding of pure and applied chemisty international conference, Srinakharinwirot Unuversity, Bangkok, Thailand. Jan. 5-7, 2011 (PACCON2011).